Engineering 59 (2026) 118–142

Contents lists available at ScienceDirect

Engineering

journal homepage: www.elsevier.com/locate/eng

Research
Low Carbon Transformation for Conventional Energies—Review

Sorption-Enhanced Catalytic Hydrogenation of Carbon Oxides by Selective Water Vapor Capture

Fiorella Massa [a], Antonio Coppola [a,*], Fabrizio Scala [b,c,*]

[a] Institute of Sciences and Technologies for Sustainable Energy and Mobility (STEMS), National Research Council (CNR), Napoli 80125, Italy
[b] Department of Chemical, Materials and Industrial Production Engineering, University of Naples Federico II, Naples 80125, Italy
[c] Faculty of Electrical Engineering and Computer Science, VŠB-Technical University of Ostrava, Ostrava 70800, Czech Republic

ARTICLE INFO

Article history:
Received 8 May 2025
Revised 6 November 2025
Accepted 26 November 2025
Available online 29 November 2025

Keywords:
Sorption-enhanced reaction
Catalytic hydrogenation
Methanation
Methanol
Dimethyl ether
Reverse water–gas-shift
Carbon capture and utilization
Power-to-fuel
Synthetic fuel
H_2O sorbent

ABSTRACT

In the energy transition context, there is growing interest in thermochemical catalytic processes for producing synthetic renewable hydrocarbons. These include biomass gasification followed by syngas conversion, or CO_2 capture from flue gases and subsequent hydrogenation—known as carbon capture and utilization (CCU). The latter uses excess renewable electricity to generate green hydrogen via water electrolysis, a concept called Power-to-Fuel. A recently proposed approach, sorption-enhanced hydrogenation, applies Le Chatelier's principle to improve reaction efficiency by selectively removing steam with a suitable sorbent. By locally adsorbing water, the system shifts equilibrium toward desired products, enabling effective hydrogenation at relatively low pressures. The key challenge is developing materials that adsorb water under relevant operating conditions yet can be regenerated without degrading the catalyst or consuming excessive energy. Most research so far has focused on fixed-bed reactors, which are simple and compact but require intermittent operation for sorbent regeneration and face heat management challenges at larger scale. In contrast, chemical looping systems using coupled fluidized beds can offer continuous operation, easier heat control, and effective sorbent regeneration. This review summarizes both early and recent developments in sorption-enhanced catalytic hydrogenation of carbon oxides into products such as methane, methanol, dimethyl ether, and carbon monoxide (via the reverse water–gas shift reaction). It covers experimental and modeling studies, and highlights key challenges and research directions for scaling up this promising technology to commercial levels.

1. Introduction

Global greenhouse gas (GHG) emissions continue to rise annually [1,2], with about 90% of carbon emissions originating from fossil fuel combustion (coal 40%, oil 32%, and natural gas 21%), 5% from cement production, and 2% from other sources [3]. According to the United Nations, current CO_2 concentrations are the highest in at least two million years [4]. These trends conflict with the Paris Agreement (COP21, 2015), which aims to limit global warming to well below 2 °C—and preferably 1.5 °C—above pre-industrial levels. Exceeding the 1.5 °C threshold is expected to trigger severe risks, including sea level rise, permafrost thawing, biodiversity loss, water scarcity, extreme weather, and food insecurity [5,6]. Despite international commitments, current measures remain far from sufficient [7].

Within the energy transition, and given the continued reliance on fossil fuels, carbon capture, utilization, and storage (CCUS) technologies are expected to play a key short- to medium-term role. However, CCUS deployment remains slow [8]. Present capture technologies are best suited for large stationary sources such as fossil fuel power plants, while CCUS is especially critical for hard-to-abate sectors—cement, steel, chemicals, and synthetic fuel production—as well as for enabling low-carbon hydrogen generation from fossil fuels, which remains a cost-effective option in several regions [8–11]. Economically, CO_2 capture accounts for about 80% of total CCUS costs. Transport, mainly via pipelines but also by road, rail, or ship, is another important factor [12]. Among storage options, geological storage is the most developed, though high costs, regulatory barriers, limited suitable sites, and weak carbon pricing mechanisms still constrain large-scale implementation [13].

* Corresponding authors.
E-mail addresses: antonio.coppola@stems.cnr.it (A. Coppola), fabrizio.scala@unina.it (F. Scala).

https://doi.org/10.1016/j.eng.2025.11.020

Carbon capture and utilization (CCU) represents a paradigm shift, turning CO_2 from a liability into a resource. Utilization pathways include both direct use—about 40% of total CO_2 demand, mainly in food and beverage industries, fire extinguishers, refrigerants, and enhanced oil recovery (EOR)—and indirect use, which dominates (~57%) through urea production in the fertilizer industry [14]. CO_2 conversion can proceed via thermocatalytic, electrochemical, photocatalytic, enzymatic, or microbial routes [8,15,16], as schematized in Fig. 1 [14].

From a technology readiness level (TRL) perspective, several CO_2-based products are already commercialized—such as urea, poly(propylene) carbonate, polycarbonates, salicylic acid, and cyclic carbonates—while others, like methanol (MeOH) and inorganic carbonates, are in the demonstration phase. Most other products, including organic acids, dimethyl ether (DME), aldehydes, alcohols, and organic carbonates, remain at the laboratory stage [17]. A key challenge is identifying the most promising processes for short- to medium-term industrial deployment [18].

Extensive research has established thermocatalytic CO_2 conversion as one of the most viable routes for large-scale industrial application [8]. Chauvy et al. [18] emphasized that converting CO_2 into platform chemicals, fuels, or energy carriers—such as methane, methanol, ethanol, DME, formic acid, carbon monoxide or syngas, gasoline, diesel, and jet fuel—could be central to achieving carbon neutrality. These reactions involve hydrogenating CO_2 to form more easily stored, transported, and utilized carbon-based products. Economically, the cost of green or low-carbon hydrogen remains the dominant factor in the overall process.

Although hydrogen is a clean, technically mature energy carrier, its large-scale deployment is still limited by high production costs. Currently, about 97% of global hydrogen comes from fossil fuels—classified as black (coal-derived) or gray (hydrocarbon-derived) hydrogen [19–22]. The production of blue (fossil-based with CCUS) and green (from water electrolysis) hydrogen is expected to grow significantly by 2030 [23–25].

In CO_2 hydrogenation for fuel synthesis, CCU technologies couple with renewable hydrogen production in power-to-fuel applications. A major challenge for renewable sources such as solar and wind is their intermittency. Converting captured CO_2 and renewable hydrogen into synthetic fuels (e-fuels) provides a means of large-scale energy storage, mitigating fluctuations in power generation and utilizing surplus electricity that would otherwise be curtailed to maintain grid stability.

1.1. CO_2 hydrogenation

Bearing in mind that carbon dioxide is difficult to activate due to its thermodynamic stability and kinetic inertness, the chemical reduction of CO_2 can be achieved via electrocatalysis, photocatalysis, or thermal catalysis [26]. Although in recent years CO_2 electroreduction is gaining attention as a path to producing multicarbon products under mild temperature and pressure, thermal catalysis is considered the most promising and effective path due to its flexibility and high versatility. The main advantages of thermal catalysis rely on higher energy efficiency, since the high temperatures can favor CO_2 activation with less energy input required, higher scalability, lower cost, and a wider range of applicable catalysts for CO_2 hydrogenation in the gas phase compared to the other paths [27].

Thermal catalysis involves a large group of reactions, such as CO_2 hydrogenation, dry reforming of methane, and nonreductive CO_2 conversion into fine chemicals. However, among the thermal catalysis possibilities, direct CO_2 hydrogenation to valuable chemicals and fuels is the most promising one [28]. By applying heterogeneous and/or homogeneous catalysts, the numerous possible products of the CO_2 hydrogenation process (Fig. 2 [29]) can be divided into two main categories: hydrocarbons and oxygenates, which consist in C1 and C1-derived products (CO, methane, MeOH, DME, and formic acid), and two or more carbon species—higher hydrocarbons, higher alcohols [29,30]. Only C1 and C1-derived products will be discussed in detail in the following sections, being such products the only ones involved in the available literature on sorption-enhanced catalytic hydrogenation.

1.2. Sorption-enhanced reactions in CCU technologies

Given the centrality of the topic related to CCU technologies, researchers have been focusing on different intensified processes for CO_2 capture and conversion by catalytic hydrogenation [31]. Numerous CO_2 capture and conversion studies have successfully applied the sorption-enhanced reaction concept, with many of the developed technologies steadily increasing their TRL.

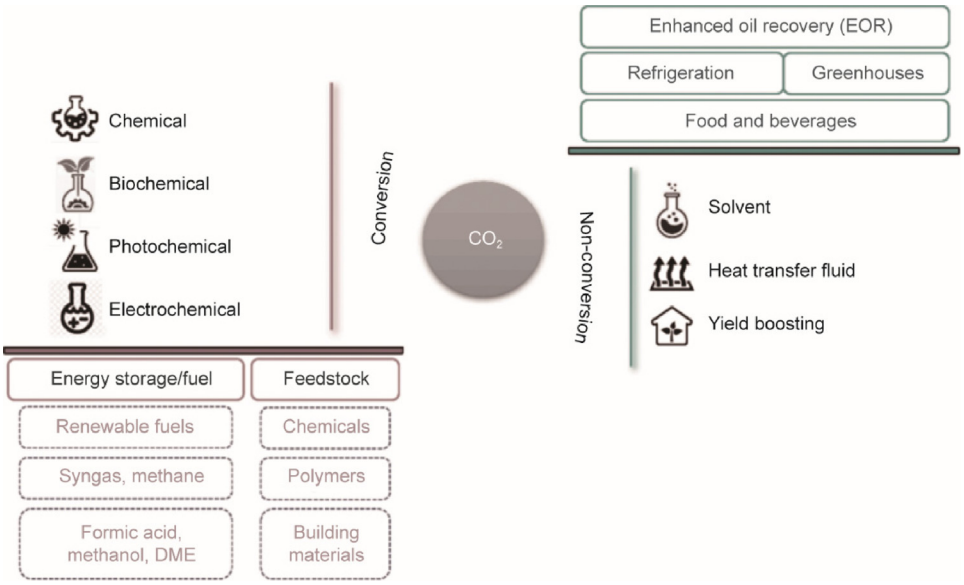

Fig. 1. Applications involving direct use of CO_2 or indirect use through conversion into other products. Reproduced from Ref. [14] with permission.

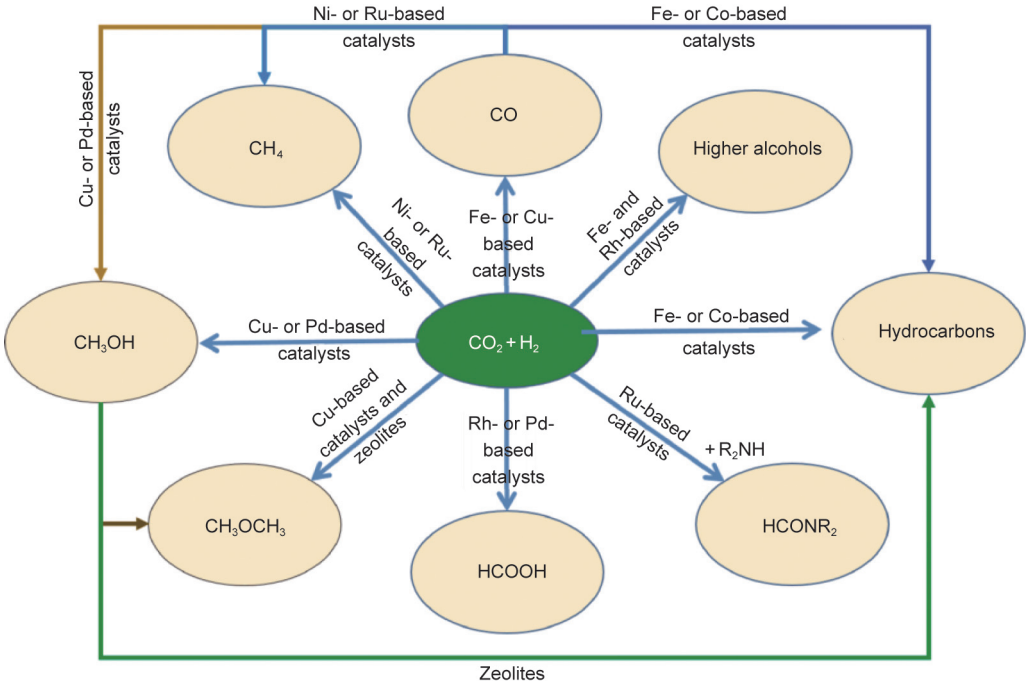

Fig. 2. CO_2 hydrogenation into hydrocarbons and oxygenates using typical metal-based catalysts. Reproduced from Ref. [29] with permission.

According to Le Chatelier principle, the conversion of an equilibrium-limited reaction can be shifted by the *in situ* removal of one of the reaction products. Additional advantages of the sorption-enhanced reactions may involve the reduced separation effort downstream of the reactor and the improved catalyst stability and selectivity [32,33].

Within the CCU technologies, sorption-enhanced processes may involve either the use of solid sorbents that capture CO_2 at medium to high temperatures (such as in sorption-enhanced gasification (SEG), sorption-enhanced reforming (SER), sorption-enhanced chemical looping, and sorption-enhanced water–gas shift (SEWGS) [32]), or the use of solid sorbents that remove the hydrogenation by-product H_2O (steam) from the reaction environment. This latter category of processes will be the focus of this review. While in principle all the CO_2 hydrogenation processes shown in Fig. 2 which produce steam as a by-product could benefit from such concept, the technologies under development for the conversion of concentrated CO_2 are primarily sorption-enhanced methanation (SEM), sorption-enhanced reverse water–gas-shift (SERWGS), sorption-enhanced DME synthesis (SEDMES), and sorption-enhanced MeOH synthesis (SEMeOHS). In terms of technological development, significant differences between the processes exist, partly connected to materials development, covering a wide range of TRLs. For SEDMES and SEMeOHS the focus is mostly on process optimization and scaling-up. In SERWGS the main goal is the development and scale-up of performing materials allowing for pressurized operation and ensuring good selectivity. SEM still requires developments on materials performance and reactor concepts, although recent investigations with commercial materials could accelerate the progress [32].

There are two primary technologies for steam separation-enhanced reactions: reactive vapor permeation (using membranes) and reactive adsorption (using solid sorbent particles). Generally, each is better suited to different process requirements (Fig. 3 [34]). Beyond shifting the reaction equilibrium, *in situ* separation can also influence catalyst deactivation, selectivity, reaction kinetics, and catalyst lifetime—effects that vary depending on the specific process. For example, removing steam *in situ* can help reduce thermally induced catalyst deactivation, which is typically accelerated at high temperatures due to elevated H_2O concentrations. In terms of operational considerations, membranes require higher steam partial pressure driving forces (greater than 1 bar) and are preferred when only modest reductions in steam levels are needed. Key factors for reactive steam permeation include hydrothermal stability and perm selectivity, while for reactive steam adsorption, high-temperature sorbent capacity and effective heat management are critical. The typical configuration for reactive steam permeation is the packed bed membrane reactor (PBMR), which combines a membrane with a catalyst-filled bed (Fig. 4(a) [33]). In cases where transfer limitations are severe, a fluidized bed membrane reactor may be employed [34].

Regarding the adsorption technology, which is widely employed for high-purity requirements in pressure swing adsorption (PSA) applications, Carvill et al. [35] were among the first to experimentally investigate reactive steam adsorption in the RWGS reaction. Overall, most literature on sorption-enhanced processes focuses on reactive adsorption. Like membrane reactors, a typical configuration for adsorption processes is the fixed bed reactor (Fig. 4(b) [33]), combined with regeneration cycles such as temperature swing, pressure swing, concentration swing, displacement regeneration, reactive regeneration, or combinations thereof. The regeneration of the adsorbent affects both the system's adsorptive capacity and catalyst performance—often with opposing effects depending on the specific reactions involved. Mass and heat transfer limitations can significantly impact these processes more than in membrane reactors. Managing the heat generated or consumed during reactions and adsorption is critical, especially for highly exothermic or endothermic reactions; for example, methanation can cause an adiabatic temperature rise of up to 500 °C. To address these challenges, several studies advocate for moving bed or fluidized bed adsorptive reactors, which offer improved heat management [34].

Zeolites are widely preferred as H_2O adsorbents. The well-defined pore sizes and geometries of these structured materials make them highly selective towards the desired adsorbate. Zeolite 3A is suitable for the removal of steam due to its pore size of 0.3

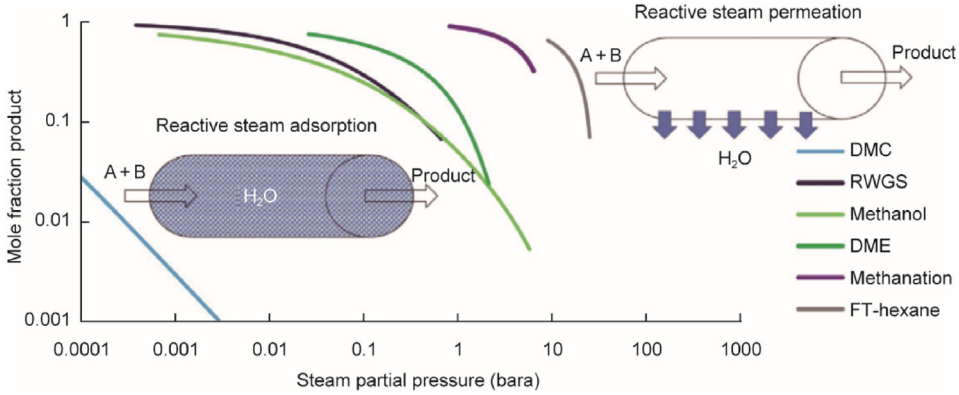

Fig. 3. Product mole fraction (CO for reverse water–gas-shift (RWGS), CH_3OH for MeOH synthesis, DME for direct DME synthesis, CH_4 for methanation, hexane for Fischer–Tropsch (FT), and dimethyl carbonate (DMC) for direct DMC synthesis) vs the partial pressure of steam. The curves are obtained through the minimization of the reaction's Gibbs free energy. Conditions: stoichiometric H_2, CO_2 feed; RWGS 300 °C, 10 bar; MeOH 250 °C, 30 bar; DME 275 °C, 30 bar; methanation 300 °C, 10 bar; FT 250 °C, 30 bar; DMC 200 °C, 30 bar. 1 bar = 10^5 Pa. Reproduced from Ref. [34] with permission.

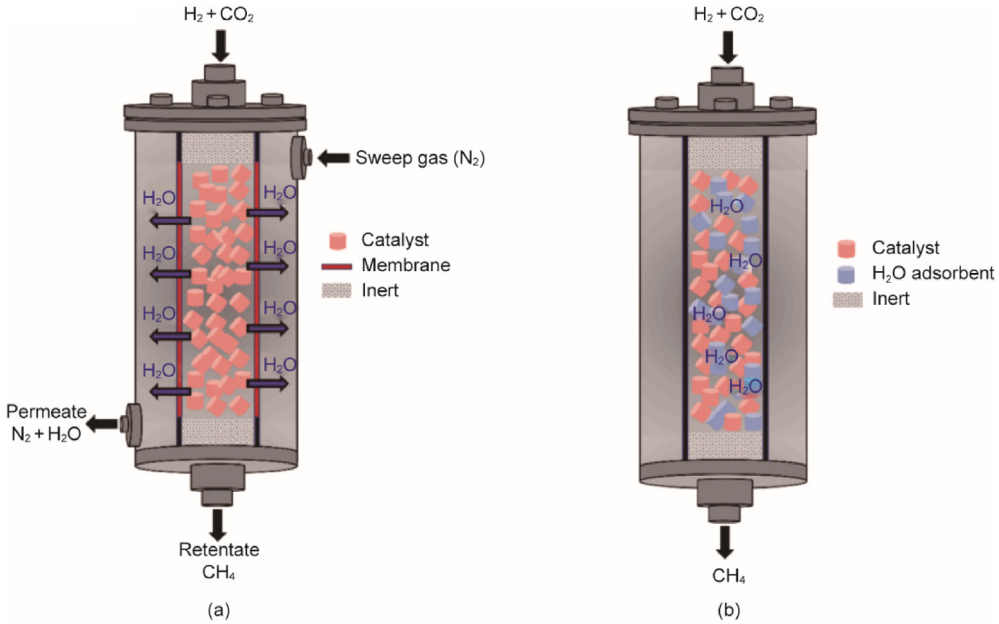

Fig. 4. Multifunctional reactors with removal of the water produced by CO_2 methanation using: (a) a H_2O-selective membrane and (b) a H_2O-selective adsorbent. Reproduced from Ref. [33] with permission.

nm that physically prevents the adsorption of slightly larger molecules. Zeolite 4A is also studied as water sorbent, however the possible co-adsorption of other components is well-known. In the presence of CO_2, in particular, a significant decrease of steam adsorption occurs despite the low adsorption capacity of CO_2 itself. For zeolite 4A, and for 5A, which is also applied for the same purposes, authors also showed co-adsorption of components such as carbon monoxide, MeOH, and DME. Other studies have highlighted that MeOH, for example, influences steam adsorption, even for zeolite 3A, thus beyond the co-adsorption. Zeolites with larger pore openings are also used: NaX for RWGS reaction and 13X when bi-functional materials are synthesized, with both catalytic and sorbent properties. Physical adsorption, characterized by low adsorption heat and activation energy, high adsorption/desorption rates and excellent reversibility, is an exothermic process with decreasing performance with temperature increase [36,37] (Fig. 5). Zeolites are used at relatively low to moderate temperatures, whereas possible steam separation enhanced reactions are typically operated at temperatures in the range 200–400 °C. Chemisorption, characterized by high adsorption heat and activation energy, may be another option to conduct a sorption-enhanced reaction, with base-metal oxides as typical chemical adsorbents. However, at medium to high temperatures, carbonates form in the presence of CO_2, making hydration less favored [34].

In the following paragraphs, a detailed review of the available literature on sorption-enhanced CO_2-conversion processes using reactive adsorption will be carried out, while membrane technology will not be considered further (the reader can refer to Ref. [34] for further details on such technology).

2. Sorption-enhanced methanation

2.1. Catalytic methanation overview

The production of synthetic natural gas (SNG) via the thermochemical route includes methanation from coal (TRL 9) or biomass (TRL levels 4–7), utilizing syngas composed of CO or CO_2/CO mixtures derived from gasification, as well as methanation of CO_2

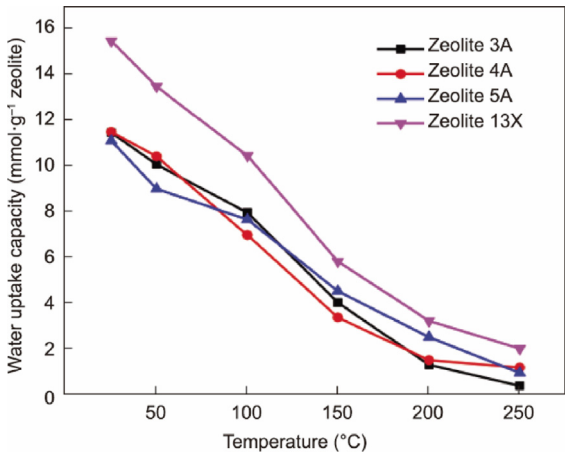

Fig. 5. Water mass uptake capacity under 20 °C saturated N_2 flow at different temperatures at 100 kPa total pressure for bead-shaped zeolites 3A, 4A, 5A, and 13X. Reproduced from Ref. [36] with permission.

within the power-to-fuel framework. This technology employs hydrogen obtained via water electrolysis and can involve the methanation of CO_2 present in biogas—produced from organic feedstock digestion (biogas upgrading)—or of waste CO_2 captured from the emissions of power plants or other industrial processes (CCU). From an economic perspective, costs for SNG production via the thermochemical pathway are primarily estimated through simulation-based economic analyses, ranging from about 0.06–0.37 EUR $kW{\cdot}h^{-1}$ SNG across various scales. Despite this wide range, significant cost reduction potential exists [38,39].

The catalytic CO and CO_2 methanation reactions were discovered by Sabatier and Senderens [40]:

$$CO_2 + 4H_2 \rightleftharpoons CH_4 + 2H_2O \qquad -165.0\,kJ \cdot mol^{-1}(@298K) \qquad (1)$$

$$CO + 3H_2 \rightleftharpoons CH_4 + H_2O \qquad -206.2\,kJ \cdot mol^{-1}(@298K) \qquad (2)$$

These reactions are highly exothermic and are characterized by a significant volume contraction, stronger for CO methanation (50%), than for CO_2 methanation (40%). Accordingly, methanation is thermodynamically favored at low temperatures (hence the need for a catalyst to enhance reaction kinetics) and at high pressures. CO_2 methanation can be considered as the linear combination of CO methanation and the reverse water–gas-shift (RWGS) reaction:

$$CO_2 + H_2 \rightleftharpoons CO + H_2O \qquad 41.2\,kJ \cdot mol^{-1}(@298K) \qquad (3)$$

The RWGS reaction typically occurs alongside methanation reactions during practical catalytic operations [38]. Among the common metals used as methanation catalysts—such as Ru, Ni, Co, Fe, and Mo—nickel is the most widely employed in commercial applications due to its high selectivity and relatively low cost [41]. For instance, Ru costs approximately 120 times more than Ni, making it unsuitable for large-scale industrial use. However, Ru is preferred for low-temperature processes because of its higher reactivity (Ni-based catalysts are only active at temperatures above 250–300 °C). While unsupported catalysts do exist, metal oxides with high surface areas are generally used as supports, including alumina (Al_2O_3), silica (SiO_2), and titania (TiO_2). Among these, Ni/Al_2O_3 catalysts are the most commonly utilized. Their performance can be enhanced with various promoters—such as MgO, V_2O_3, La_2O_3, and CeO_2—which improve activity, thermal stability, and resistance to carbon deposition (coking). It is important to note that selecting a commercial catalyst is a complex decision, as these materials are vulnerable to various deactivation mechanisms, including chemical, thermal, and mechanical factors. The primary cause of chemical deactivation in commercial Ni-based catalysts is carbon (coke) accumulation on the catalyst surface [42]. Most kinetic studies to date have focused on CO methanation, and there is currently no universally accepted kinetic model in literature. Among the most influential contributions, Xu and Froment [43] developed a widely cited model addressing steam methane reforming, CO/CO_2 methanation, and water–gas-shift (WGS) kinetics. In the context of CO_2 methanation, a comprehensive review was conducted by Gao et al. [44]. Two primary mechanisms have been proposed for CO_2 methanation over nickel-based catalysts. The more widely accepted mechanism involves the dissociative adsorption of CO_2 on the catalyst surface, forming CO and O. An alternative pathway suggests the direct hydrogenation of CO_2 through carbonate or formate intermediates, bypassing CO formation [45]. These mechanisms are summarized in Fig. 6 [45]. For methanation of CO_2 over Ni catalysts, it is generally observed that small quantities of CO can inhibit the reaction, as CO tends to preferentially adsorb on the Ni surface, outcompeting CO_2. Moreover, recent experimental studies indicate that H_2O also significantly suppresses the methanation rate by acting as an inhibitor [46].

In industrial practice, catalytic methanation is commonly used in ammonia synthesis plants to eliminate carbon monoxide. Beyond this established application, research into SNG production started in the United States during the 1960s—an era marked by the growing reliance on natural gas. Interest in SNG technologies expanded over the following decades, driven initially by the oil crisis and later by increasing environmental awareness. Kopyscinski et al. [47] reviewed various SNG production pathways from coal and biomass, highlighting the numerous commercial methanation processes already in place. These industrial processes typically employ a series of catalytic adiabatic fixed beds, operating between 250 and 600 °C and under high pressures. Intermediate cooling steps, gas recirculation, and steam injection into the first reactor are standard features, primarily to mitigate carbon deposition [41]. As a typical example, the layout of one of the most recognized systems, the Topsøe's recycle energy efficient methanation process (TREMP), is illustrated in Fig. 7 [47]. Moreover, the fluidized bed technology was also proposed to innovate the process, being the technology favorable for the management of highly exothermic reactions at the industrial scale [48]. An alternative approach to SNG production, known as liquid-phase methanation (LPM), was also investigated. This process involved a three-phase fluidized-bed reactor, where catalytic methanation occurred in the presence of a circulating mineral oil that served to absorb the exothermic reaction heat. However, experimental results revealed low conversion rates and significant catalyst losses, leading to the discontinuation of further research in this direction [38].

Turning to CO_2 methanation, most of the power-to-gas (PtG) projects are located in Germany, United States, Denmark, and Canada. The PtG concept was first suggested by Koji Hashimoto

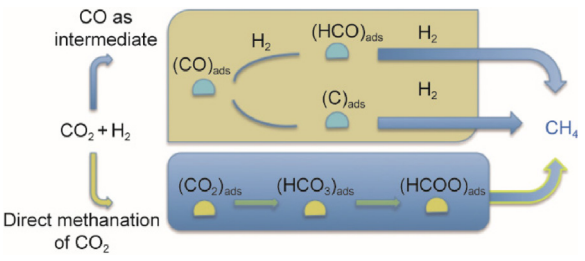

Fig. 6. Simplified reaction mechanisms of CO_2 methanation. ads: adsorbed. Reproduced from Ref. [45] with permission.

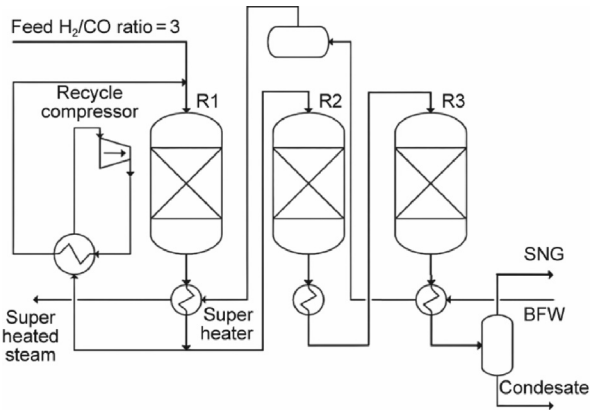

Fig. 7. The TREMP scheme. R1–R3: reactors; BFW: boiler feed water. Reproduced from Ref. [47] with permission.

in 1994 to use surplus energy from renewable sources and convert it into the chemical energy of a combustible gas like H_2 (power-to-hydrogen (PtH)) or CH_4 (power-to-methane (PtM)) [33]. The first projects started in 2004 and involved the production of H_2. However, subsequent projects considered more favorable the production of other gaseous fuels, such as methane, taking advantage of its social acceptance and already well-developed infrastructure. Methane could be directly injected into existing gas infrastructure if the H_2 at the outlet of the process met the grid specification. So far, the standards for the hydrogen maximum content are not the same worldwide, and, although a maximum of 20% is considered technically feasible, the fixed limit value is generally around 5% in volume. The first project of PtM with catalytic methanation was launched in 2009 in Germany, which is the country leading the PtG projects growth and where 68% of the projects identified in 2020 (220 in 20 European countries) were located [33]. A prominent example in Germany is the PtG plant located in Werlte, which produces synthetic methane and injects it into the natural gas grid [9,33]. Known as the Audi e-gas plant, it is the largest industrial-scale PtG facility worldwide, with an annual output of approximately 1000 tons of synthetic methane.

2.2. Thermodynamics of SEM of CO_2

The strong exothermicity of the methanation reactions, together with the reduction in the number of moles, entail a theoretical high yield at low temperatures and high pressures, although kinetic limitations represent a counteracting effect to be considered. For methanation, thus, the sorption-enhanced process is essentially proposed to improve the performance at low pressures and medium temperatures, overcoming the thermodynamic constraints. The pressure reduction implies a net decrease in the energy duty for gas compression work which, if done downstream the process, would involve a lower volumetric flow rate [35]. The concept was also proposed to enhance the utilization of excess heat generated by the reaction, as the primary efficiency loss in the Sabatier process stems from heat release, which accounts for approximately 17% of the heating value.

While traditional CO/CO_2 methanation was deeply studied in various thermodynamic studies [49–52], the extension to SEM conditions was almost unexplored up to the work by Faria et al. [53] in 2018, reporting the thermodynamic analysis for SEM applied to biogas upgrading. The study highlighted for the first time one of the most sensitive aspects of working under SEM conditions (i.e. the possible solid carbon deposition), which is already one of the main challenges during operation of traditional CO methanation reactors, leading to catalyst deactivation. In fact, previous thermodynamic studies showed that carbon deposition could be extensive during CO methanation, but usually not during CO_2 methanation [50–53]. However, the increased importance of the carbon-generating reactions due to the H_2O removal, makes CO_2 methanation under SEM conditions affected by the phenomenon of possible coke formation. The study by Faria et al. [53] investigated temperatures and pressures between 200–450 °C and 1–30 atm, respectively, different biogas compositions and different water removal fractions. The sorption-enhanced effect was confirmed, with water removal increasing the CH_4 yield but only up to an optimum value, above which, coke formation was favored. Water removal can also be useful to minimize the production of CO_x, allowing to comply with the biogas quality specifications for injection into the natural gas grid. The target of achieving, by means of SEM conditions, SNG purity sufficient for the natural gas grid specifications, was also the focus of the work by Massa et al. [54], concerning thermodynamics of pure CO_2 SEM at low pressure (1–10 atm). The analysis, which detailed the carbon deposition limits for this system using ternary diagrams (Fig. 8 [54]), revealed that while SEM conditions offer advantages, steam removal can lead to substantial carbon formation—particularly at high temperatures and low pressures—making partial steam retention preferable when using a stoichiometric CO_2/H_2 feed. The authors also identified an optimal H_2O removal fraction at each temperature and pressure that maximizes performance while minimizing carbon formation. Regarding gas quality, the H_2 content in the product emerges as the most critical constraint to be maintained (Fig. 9 [54]).

In 2021, Hashemi et al. [55] performed a thermodynamic study investigating the effect of intermediate water removal on the CO_2 conversion in an isothermal fixed bed reactor schematized as one-dimensional pseudo-homogenous model and considering either pure CO_2 or a feed of CO_2 and methane as a typical biogas mixture. The analysis illustrated the importance of the reactor length to the optimal water removal point, demonstrating that this length may not be close to the equilibrium length when water removal is carried out to obtain the best performance. The study pushed towards other concepts such as partial water removal and partial reactant feeding along the reactor to control the reaction rate and lead to efficient heat management [55].

Overall, all the cited literature helped to highlight how continuous membrane reactors or dual fluidized bed reactors appear to be more suitable for flexible and carbon-free operation, unlike fixed bed reactors. In fact, in fixed beds all the water produced is subtracted until sorbent saturation, and this fact combined with reaction kinetics and transport phenomena, might significantly increase the local carbon formation, especially in transient operation [54].

2.3. SEM of CO_2: Early studies

2.3.1. General considerations on configuration and materials

A list of the research studies available in the literature on SEM is reported in Table 1 [56–80]. As in conventional methanation, SEM has so far mostly been proposed in the configuration of fixed bed reactors. However, contrary to conventional methanation, the SEM process in this configuration cannot be carried out under steady state conditions, since the H_2O sorbent must be regularly regenerated once saturated. In adsorption-based processes, regeneration mode is a crucial choice influencing the reactor configuration. The most widely used regeneration approaches in fixed beds are the vacuum swing adsorption (VSA) and the PSA, since the low heat transfer rate makes the temperature swing adsorption (TSA) less performing. Apart from the difficult temperature control, the main drawback of such fixed bed reactor schemes is the inherently

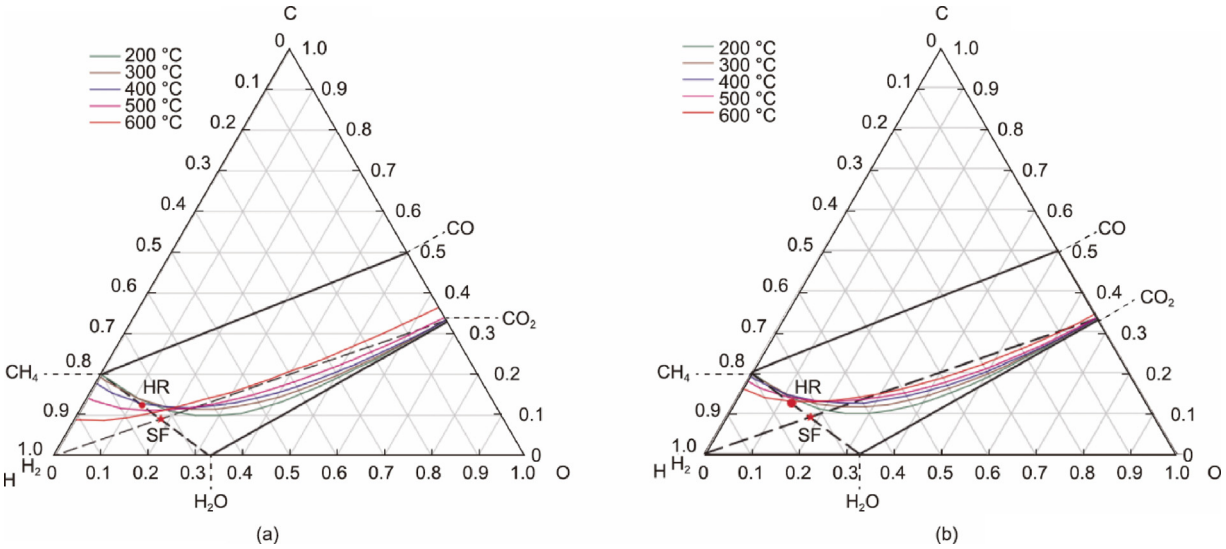

Fig. 8. C–H–O ternary diagrams with carbon deposition boundaries at different temperatures (200–600 °C), at (a) 1 atm and (b) 10 atm. SF: stoichiometric feed; HR: SEM condition with removal of half of the maximum generated steam. Reproduced from Ref. [54] with permission.

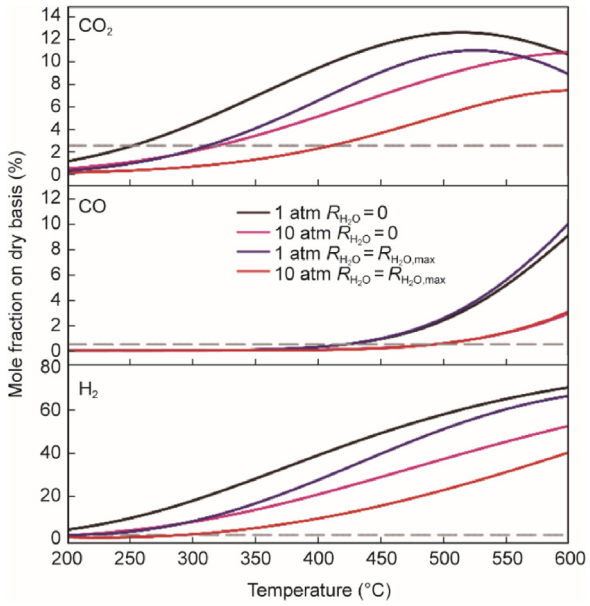

Fig. 9. Molar fraction of CO_2, CO, and H_2 (dry basis) vs temperature at two pressures (1 and 10 atm), at stoichiometric feed, under traditional methanation (R_{H_2O} = 0) and optimal SEM (R_{H_2O} = $R_{H_2O,max}$), corresponding to the fraction maximizing performance while avoiding carbon formation. Reproduced from Ref. [54] with permission.

discontinuous operation, implying cyclic switching of the gas flows feeding the reactors, and additional purge phases (to avoid contamination of the streams). When using fixed bed reactors for continuous gas processing, a cluster of reactors is required, along with numerous valves and intricate piping systems to perform the various steps involved in the process. The control of multiple transient reactors makes the fixed bed reactors configuration relatively complex to be operated.

Many studies, as we will also see later for the other sorption-enhanced processes, address the issue of materials development, both catalysts and sorbents, which need to be sufficiently performing. These two materials can be either used in a mixture or as bi-functional materials combining catalytic and sorbent properties on the same particles, the latter being the case most frequently found in the literature. The preparation methods influence the catalyst activity and selectivity since the active metal dispersion, particle size, acidity, and interaction with the support vary if considering different methods. There are two types of preparation routes for bi-functional materials: the mixing and shaping (physical mixture) and the catalytic metal loading (chemical) ones. Mixing and shaping is the easiest route, as all possible catalyst preparation methods can be utilized, such as impregnation, ion-exchange, deposition, precipitation, and co-precipitation. A sufficiently active catalyst can be physically mixed to a sorbent and pelletized to obtain the material for the SEM process. However, the pelletization procedure can cause mechanical stability issues and pore blockage can significantly decrease the surface area of the material. Although the mixing and shaping route is very flexible, being in sorption-enhanced CO_2 methanation the proximity of sorption and catalytic sites fundamental, direct loading into the support is suggested. Ion exchange is typically used with the active metal exchanged with the Na^+, K^+, and Ca^{2+} of a zeolite framework. Impregnation is another traditional catalyst preparation method, where the metal precursor is dissolved in a measured volume of distilled water, allowing the solution to infiltrate and fill the pores of the support material [37].

2.3.2. Studies on bi-functional and mixed Ni/zeolite materials

In 2013, Borgschulte et al. [56] began investigating the enhancement of CO_2 methanation through sorption-enhanced catalysis. This approach involved the application of nickel onto zeolite 5A particles via ion exchange. Catalysts with a nickel loading of approximately 6 wt% demonstrated the best performance. To assess the effectiveness of the sorption-enhanced system, the researchers compared it to a commercial catalyst. The modified catalyst exhibited improved selectivity and maximum conversion at reduced temperatures. The sorption effect was confirmed through transient kinetic measurements. Initially, a 100% methane yield was observed. However, this yield declined once the amount of water generated during the reaction surpassed the zeolite's adsorption capacity, leading to water breakthrough in the reactor effluent. The system maintained 100% selectivity for a limited period, after which catalyst regeneration was necessary to restore performance (Fig. 10 [56]).

In subsequent years, the same authors continued to advance their research in this field. By investigating catalysts prepared

Table 1
Main studies on SEM.

Catalyst/sorbent	Reactor type	Feed comp. (vol%) $H_2/CO_2/N_2/CH_4$	SE Temp. (°C)	Regen. Temp. (°C)	Press. (bar)	GHSV	Sample mass (g)	H_2O upt. ($mmol \cdot g^{-1}$)	Max. conversion	Max. CH_4 selectivity	Refs.
Experimental studies											
Ni/zeolite 5A (bi-functional)	Tubular flow	88.9/11.1/0/0	130–300	N.A.	1.2	1 000 h^{-1}	13	N.A.	~100% (CO_2)	100%	[56]
Ni/zeolite 3A & 5A (bi-functional)	Tubular flow	88.9/11.1/0/0	130–350	N.A.	1.2	1 000 h^{-1}	13	N.A.	~100% (CO_2)	~100%	[57]
Ni/zeolite 5A (bi-functional)	Plate cell	80/20/0/0	270–320	270–320	N.A.	N.A.	N.A.	N.A.	~100% (CO_2)	~100%	[58]
Ni-Al_2O_3/zeolite 4A (mixed)	Fixed bed	9.9/2.5/6.0/81.6	250–350	350–450	1	2 500 h^{-1}	0.6 (cat.) + 3.0 (sorb.)	0.98–2.0	~100% (H_2 & CO_2)	100%	[59]
Ni/zeolite 5A & 13X (bi-functional)	Fixed bed	80.2/19.8/0/0	300	300	1	92 h^{-1}	250	N.A.	100%	100%	[60]
Ni/zeolite 5A (bi-functional)	Thermo-balance	80/20/0/0	320–500	320–500	1	N.A.	2.5–3	N.A.	N.A.	N.A.	[61]
Ni-CaO-Al_2O_3/ zeolite 4A (mixed)	Fixed bed	55.3/16.7/28/0	290	290–700	15	23 000 mL·$(g_{cat} \cdot h)^{-1}$	1.4 (cat.) + 5–16 (sorb.)	1.39	92%–94% (H_2)	100%	[62]
Ni-CaO-Al_2O_3/La_2O_3 (mixed)	Fixed bed	55.3/16.7/28/0	290	290–700	15	23 000 mL·$(g_{cat} \cdot h)^{-1}$	1.4 (cat.) + 5–16 (sorb.)	0.5	92%–94% (H_2)	100%	[62]
Ni-CaO-Al_2O_3/CaO (mixed)	Fixed bed	55.3/16.7/28/0	290	290–700	15	23 000 mL·$(g_{cat} \cdot h)^{-1}$	1.4 (cat.) + 5–16 (sorb.)	4	92%–94% (H_2)	100%	[62]
Ni-Ce/zeolite 13X (bi-functional)	Fixed bed	10/2.5/6/81.5	180–320	300–450	1	714–923 mL·$(g_{cat} \cdot h)^{-1}$	6.5–8.4	0.3–1.65	98%–100% (CO_2)	100%	[63]
Ni/zeolite 13X & 5A & L (bi-functional)	Fixed bed	10/2.5/6/81.5	180–320	300–450	1	714–923 mL·$(g_{cat} \cdot h)^{-1}$	6.5–8.4	0.3–1.65	98%–100% (CO_2)	100%	[63]
—/CaO (hydration/ dehydration)	Fluidized bed	0/10/80/0	200–300	350–450	1	N.A.	10	0.3–2.7	N.A.	N.A.	[64,65]
—/zeolite 3A (hydration/ dehydration)	Fluidized bed	+ 10% H_2O	200–300	350–450	1	N.A.	10	0.3–2.7	N.A.	N.A.	[64,65]
Rh/zeolite 5A (mixed)	Fixed bed	80/20/0/0	250–275	375–400	1	1 500–2 570 mL·$(g_{cat} \cdot h)^{-1}$	0.35 (cat.) +1.75 (sorb.)	2–6	92%–100% (H_2)	100%	[66,67]
Rh/zeolite 3A & 4A & 13X (mixed)	Fixed bed	75/25/0/0, 80/20/0/0, 83.3/16.7/0/0	275	400	1	230–300 mL·$(g_{cat} \cdot h)^{-1}$	0.35 (cat.) +1.05–1.75 (sorb.)	1–5	90.1%–95.7% (H_2) 87.8%–98.7% (CO_2)	100%	[68]
Ni/zeolite 4A (mixed)	Fixed bed	80/20/0/0	250	400	1	509 mL·$(g_{cat} \cdot h)^{-1}$	0.35 (cat.) +1.4 (sorb.)	5.3	99.7% (H_2)99.8% (CO_2)	100%	[69]
Ni/zeolite 4A (mixed)	Fixed bed	73/9/4/0, + 14% CO	230	230–300	1–10	200–2 000 h^{-1}	20 (cat.) +80 (sorb.)	0.06–0.144	100% (H_2 & CO_2)	~100%	[70]
Ni/zeolite 4A (mixed)	Fixed bed	69–84/8–24/0/0, + 0–18% CO	225–250	400	10	150–300 h^{-1}	20 (cat.) +80 (sorb.)	0.06–0.144	100% (H_2 & CO_2)	100%	[71]
Ni-Fe-Al_2O_3/zeolite 5A (mixed)	Fixed bed	80/20/0/0, 54.6/13.6/0/31.8	250–400	250–500	1	60 000 mL·$(g_{cat} \cdot h)^{-1}$	0.25 (cat.) +10.25 (sorb.)	N.A.	94% (CO_2)	~100%	[72]
Simulation studies											
Ni/zeolite 13X (bi-functional)	Fixed bed	80/20/0/0	280–320	340	1.5–10	400 h^{-1}	N.A.	1–2	N.A.	N.A.	[73,74]
Ni-SiAl/zeolite 3A (mixed),	Fixed bed	80/20/0/0	250–350	250–350	1	N.A.	N.A.	N.A.	99.7% (CO_2)	99.9%	[75]
Ni-SiAl/zeolite 3A (mixed) Ni-Al_2O_3/zeolite 3A (mixed)	Fixed bed	60/15/0/23, + 2% H_2O	200–350	200–350	1	N.A.	N.A.	N.A.	99.6% (CO_2)	~100%	[76]
Ni-Al_2O_3/CaO (mixed)	Fluidized bed	38–80/0–33/0/0–43, + 0–50% CO	250–350	450	1	N.A.	N.A.	N.A.	~100% (H_2 & CO_2)	~100%	[77,78]
Ni/zeolite 13X (bi-functional)	Fixed bed	16/4/0/80	280–320	N.A.	1	500 mL·$(g_{ads} \cdot h)^{-1}$	1284	N.A.	~100% (H_2 & CO_2)	~100%	[79,80]

GHSV: gas hourly space velocity; comp.: composition; SE Temp.: sorption enhanced temperature; upt.: uptake ; Max.: maximum; N.A.: not available; cat.: catalyst; sorb.: sorbent; g_{cat}: grams of catalyst; g_{ads}: grams of adsorbent (bifunctional) material.

via ion exchange of a nickel nitrate solution into two zeolites with differing pore sizes, they demonstrated that the kinetics of the methanation reaction depended on the nanostructure of the catalyst-sorbent system. The systems with different pore sizes presented different Ni-particles size distributions. Through a microstructural characterization of the catalyst, they observed that the selectivity to methane was greatly enhanced if the zeolite pore size was larger than 5 Å, while pore sizes of less than 3 Å, thus Ni on 3A zeolites, resulted in a lower overall conversion rate and selectivity. The Ni/zeolite 3A bi-functional material was more performing as low temperature catalyst for the RWGS reaction to produce carbon monoxide [57]. In view of possible new reactor concepts required for the SEM process, Borgschulte et al. [58] also measured the spatial water distribution in a fixed bed reactor using time resolved neutron imaging and the product gas by Fourier transform infrared spectroscopy (FTIR)–gas analysis. They identified a reaction front running through the reactor with the conversion rate starting to decrease as the front reached the exhaust, an effect that must be considered for the design of large-scale fixed bed reactors [58].

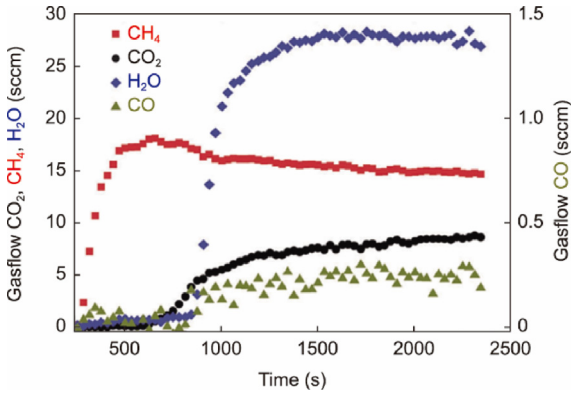

Fig. 10. Time evolution of the gas composition at the sorption-enhanced fixed bed methanation reactor outlet over time (T = 170 °C, 20 cm^3 STP·min^{-1} CO_2, 13 g Ni sorption catalyst). sccm: standard cubic centimeters per minute; STP: standard temperature and pressure. Reproduced from Ref. [56] with permission.

One of the most influential contributions to the field was published by Walspurger et al. [59] in 2014. The authors investigated SEM as a method for upgrading SNG, which has been the most frequently explored application of SEM in literature, particularly in earlier studies. Their work highlighted the significant improvements in methane purity achievable through this approach, while also identifying the process limitations from both experimental and thermodynamic perspectives. The SEM process demonstrated outstanding performance to produce high-grade SNG at low pressures, using commercially available materials. These findings underscore the potential of SEM to enhance gas quality in upgrading processes (Fig. 11 [59]).

The thermodynamic behavior of CO_2 methanation was analyzed using Aspen Plus, considering typical industrial conditions such as stream compositions, recycle ratios, and inlet and maximum reactor temperatures. The modeled process configuration was a series of three fixed bed reactors, with intermediate cooling between the reactors, and a recycle from the second to the first reactor. To assess the impact of *in situ* water capture, the third methanator was modeled in two variants: as a traditional methanation reactor and as a SEM reactor. The goal was to produce SNG of sufficient quality to meet specific gas grid injection standards, with particular attention to the outlet hydrogen concentration, which must remain below 0.5%. Additional target specifications included CO_2 < 3%, CO < 0.5%, and H_2O < 90 ppm at a system pressure of 60 bar. Replacing the third conventional reactor with a SEM unit resulted in a notably lower hydrogen content in the final SNG stream. This configuration enabled compliance with gas grid specifications at significantly reduced operating pressures (Fig. 12 [59]).

The authors emphasized that operating at pressures lower than those typically used in conventional methanation processes—since feed streams are generally supplied at pressures below 10 bar—can result in substantial energy savings from reduced compression requirements. Specifically, compression energy savings of up to 60% were estimated at an operating pressure of 5 bar. As previously discussed, placing the compression stage downstream of the methanation process, rather than upstream, significantly reduces the volumetric flow rate to be compressed, thereby lowering energy consumption. When evaluating operational pressures around 25 bar, the inlet composition of a SEM reactor placed downstream of two conventional reactors (in a configuration with a recycle) would only imply a modest temperature rise during methanation. In contrast, at pressures below 10 bar, the increased amounts of CO_2 and H_2 entering the third reactor would cause a much larger temperature rise during the reaction. This thermal challenge highlights the need to explore alternative reactor designs specifically tailored for low-pressure SEM processes.

The experimental activity of Walspurger et al. [59] consisted in testing a zeolite 4A physically mixed and pelletized with a Ni-based catalyst. Under thermodynamically unfavorable conditions (i.e. at low pressures and, in the specific case of these experiments, at temperatures above 400 °C), the methanation reactions were disadvantaged to such an extent that, considering biogas feeding, methane consumption occurred. Overall, the commercial materials could operate in cyclic sorption-enhanced conditions, with breakthrough water capacities of 1.52, 1.31, and 1.07 mmol·g^{-1} at 250, 300, and 350 °C, respectively. The regeneration procedure, which involved a temperature-swing cycle using purge gas, had minimal impact on the sorbent's uptake capacity. Additionally, the temperature of regeneration could be selected close to the adsorption operating conditions, ensuring efficient cycle performance.

Later, Delmelle et al. [60] expanded their study to include zeolite 13X in addition to zeolite 5A. The catalysts were prepared by wet impregnation, resulting in the homogeneous distribution of nickel nanoparticles throughout the support, with particle sizes ranging from 20 to 30 nm. The 5Ni/13X catalyst demonstrated activity across a wide range of reduction temperatures, showing already significant activity at 300 °C. In contrast, nickel particles supported on zeolite 5A were only reduced above 500 °C, as observed in temperature programmed reduction (TPR) experiments (Fig. 13 [60]). This finding has important implications for catalyst selection, particularly in SEM processes, which typically operate optimally at temperatures not exceeding 300 °C. Zeolite 13X exhibited an operational lifespan three times longer than zeolite 5A, attributed to its larger water sorption capacity, especially at temperatures above room temperature. Despite similar CO_2 conversion performance in conventional CO_2 methanation for both bi-functional materials, the 5Ni/13X catalyst delivered the best overall performance. The larger pores of zeolite 13X (9 Å) entailed better transport of air and water, which in turn facilitated more efficient catalyst regeneration under oxidizing conditions. This is because O_2 and N_2 molecules are of a similar size and mass to water molecules, making collisions more effective between these species. Consequently, air is more efficient than hydrogen at carrying water out of zeolite during regeneration.

Delmelle et al. [61] also investigated the long-term stability of a Ni-based catalyst supported on zeolite 5A for SEM, specifically focusing on water diffusion as the rate-limiting step in both the methanation and drying phases during cyclic treatments. While the relatively mild conditions of SEM, compared to conventional methanation processes, generally promote stable catalyst activity with no significant long-term deactivation, a specific degradation mechanism was observed over multiple methanation/drying cycles. The samples subjected to cyclic treatments exhibited carbon contents approximately 55% higher than those treated under continuous methanation conditions. This increase in carbon deposition was linked to the formation of intermediates and products within the zeolite, which partly blocked the catalyst pores. As a result, water diffusion during the drying phase was hindered, leading to a 40% reduction in the diffusion coefficient after 40 cycles. This reduction in water diffusion lengthened the regeneration process, although it did not impact on the catalytic performance. The authors suggested that drying in oxidizing conditions could mitigate this degradation effect [61].

2.3.3. Studies on sorbents other than zeolites

In 2021, Agirre et al. [62] examined the most suitable parameters for performing SEM in fixed bed reactors to achieve the lowest possible reaction temperature while maintaining high methane selectivity and minimizing CO production. Their findings indicated that an optimal operating temperature of 290 °C and a total

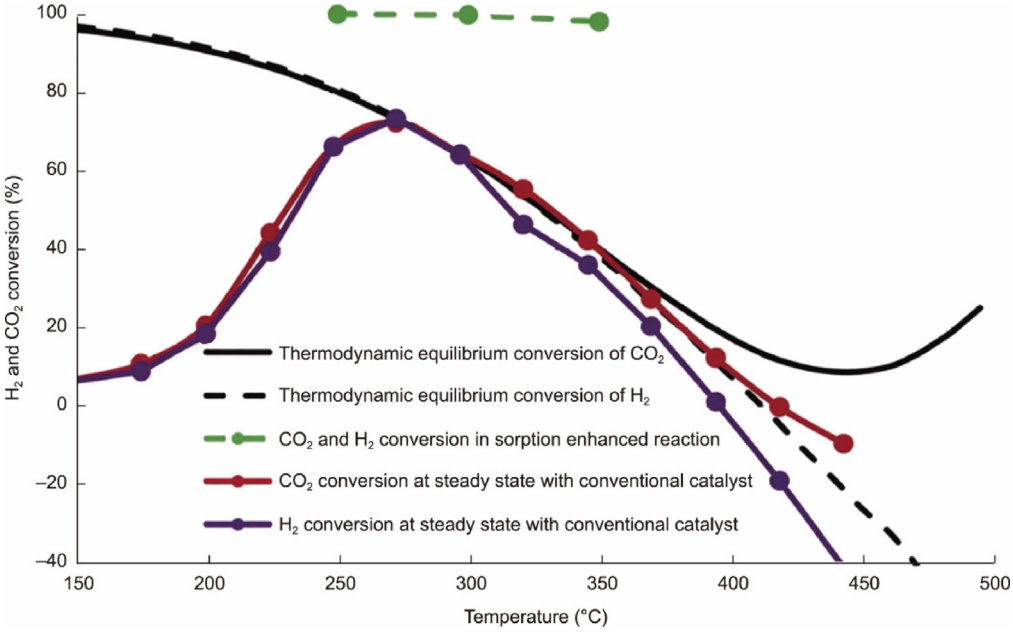

Fig. 11. CO_2 and H_2 conversion in a fixed bed under traditional methanation (red and violet lines) as a function of temperature at atmospheric pressure using a conventional Ni-based catalyst, compared to CO_2 and H_2 conversion under SEM conditions (green line) using a zeolite 4A adsorbent. Black curves refer to thermodynamic equilibrium conversion (inlet composition: 2.4% CO_2, 9.4% H_2, 77.8% CH_4, 4.7% H_2O, and 5.6% N_2). Reproduced from Ref. [59] with permission.

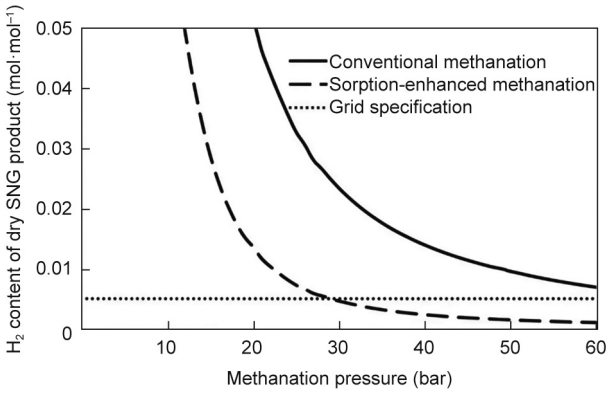

Fig. 12. H_2 concentration in SNG produced from conventional methanation and SEM. Reproduced from Ref. [59] with permission.

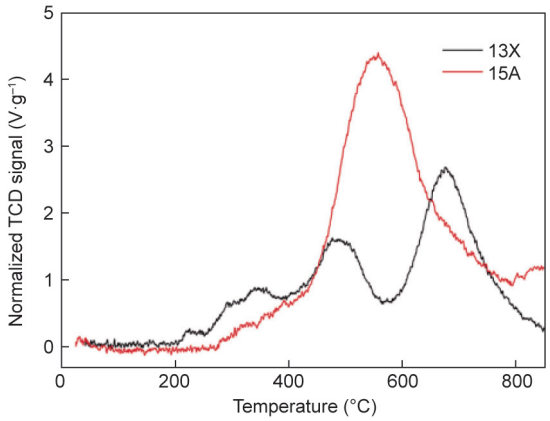

Fig. 13. H_2-TPR profiles of 5Ni/13X and 5Ni/5A. TCD: thermal conductivity detector. Reproduced from Ref. [60] with permission.

pressure of 15 bar resulted in hydrogen conversions of 92%–94%, with no detectable CO. The study utilized a commercial catalyst (KATALCO-57-4Q by Johnson Matthey), which was physically mixed with the sorbent and showed activity above 275 °C. In addition to zeolite 4A, the authors also evaluated two other sorbents—calcium oxide (CaO) and lanthanum oxide (La_2O_3). Zeolite exhibited rapid water adsorption and reached saturation quickly, resulting in a short transient period, which can be a critical limitation when coupled with methanation kinetics. At room temperature, zeolite could adsorb approximately 11 wt% of water, but its capacity significantly declined with increasing temperature, limiting its effectiveness at typical methanation conditions. In contrast, CaO demonstrated effective water adsorption up to 350 °C, indicating a fundamentally different behavior due to the expected chemisorption mechanism. While the initial room temperature sorption capacity of CaO exceeded that of zeolites, its performance degraded after the first cycle. From the second cycle onward, the sorption capacity decreased, and the process appeared to become partially irreversible—unlike the reversible sorption behavior observed with zeolites. Wei et al. [63] further investigated the performance of four different bi-functional catalyst–sorbent materials in fixed bed configurations. Among them, the most effective formulation was a 5 wt% Ni catalyst supported on zeolite 13X—recognized as superior to zeolite 5A for SEM—enhanced with 2.5 wt% cerium. This material exhibited excellent performance, achieving 100% methane selectivity and full conversion at temperatures as low as 180 °C, along with good stability over repeated reaction–regeneration cycles.

Coppola et al. [64,65] proposed a novel process configuration based on the concept of chemical looping in dual interconnected fluidized bed systems to perform in one reactor the SEM process (methanation/hydration) and continuously regenerate the saturated sorbent in the other reactor, to overcome the intrinsic discontinuous operation of fixed bed reactors (Fig. 14 [65]). The authors tested the performance of two possible sorbents in terms of hydration and dehydration cycles (Fig. 15 [65]) at different operating conditions, relevant for catalytic methanation, in a lab-scale interconnected fluidized beds system, considering the temperature

effect and the presence of CO_2 in the reaction environment. The sorbents were CaO obtained from natural limestone, chemically reacting with H_2O to form $Ca(OH)_2$, and an attrition-resistant spherical 3A zeolite. Although for the zeolite, presenting quite stable behavior over multiple cycles, CO_2 competed with H_2O for adsorption, the presence of CO_2 for CaO had a much more dramatic effect, due to the irreversible carbonation of the sorbent. However, despite the better asymptotic capture capacity of zeolites, other aspects such as the higher cost of these materials need to be considered.

More recently, García et al. [66] investigated the reaction kinetics for CaO when applied as a sorbent in the SEM process, thus under operating conditions such as atmospheric pressure and temperatures between 200 and 350 °C. The impact of simultaneous hydration and carbonation reactions, successfully modeled by a shrinking core model with chemical reaction control and investigated in a wide range of H_2O and CO_2 concentrations (i.e. 5–20 vol%), resulted in the reduction in hydration capacity in the presence of CO_2, even in small quantities, due to the irreversible formation of a $CaCO_3$ product layer. The mechanism of such deteriorative effect, already observed in other works, still needs deeper research to be completely understood.

2.4. SEM of CO_2: Latest advances in materials development

Since 2022, the literature production on this subject has experienced a new phase of growth, mainly due to few groups of researchers who have focused their activity on the study of the SEM process. Gómez et al. [67] studied SEM at atmospheric pressure for stoichiometric H_2/CO and H_2/CO_2 gas mixtures, as well as for a syngas containing H_2, CO, and CO_2 under stoichiometric proportions, using a fixed bed of Rh-based catalyst mixed with a commercial zeolite 5A. Pure CH_4 production was achieved at 275 °C for sorption-enhanced CO_2 methanation at space velocities of up to 514 $mL_{CO_2}\cdot(g_{cat}\cdot h)^{-1}$, while under the same conditions, 86 vol% of CH_4 was obtained for SEM of CO, with a lower space velocity, equal to 440 $mL_{CO}\cdot(g_{cat}\cdot h)^{-1}$ (Fig. 16 [67]). Lower CH_4 purity, about 60%, was obtained when both carbon oxides were present in the feed gas, suggesting that lower space velocities for CO and CO_2 or alternative adsorbents could allow for better performance in the case of a CO/CO_2 mixture [67].

In a successive work, Gómez et al. [68] analyzed several commercial zeolites (3A, 4A, 5A, and 13X) physically mixed with a Rh-based catalyst to perform CO_2 SEM, demonstrating that zeolite 4A was the most suitable zeolite resulting in the highest CH_4 purity (85% at 275 °C and with a gas space velocity of 230 $NmL\cdot(g_{cat}\cdot h)^{-1}$) and pre-breakthrough period (22 min), compared to the others. Under the best detected operational conditions, the CO_2 conversion increased from 45.2% in conventional methanation up to 94.5% under SEM conditions. The materials, regenerated through a temperature swing process, showed good stability over 10 consecutive SEM/regeneration cycles, giving repeatable results (Fig. 17 [68]).

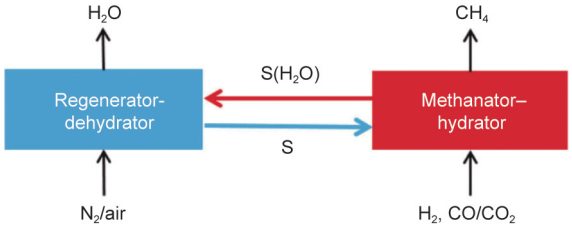

Fig. 14. Scheme of the chemical looping SEM concept. Reproduced from Ref. [65] with permission.

The same authors then analyzed via *in situ* FTIR measurements also Ru and Ni besides rhodium as active catalytic phases. The species formed on the catalyst surface and in the gas phase during CO_2 methanation and SEM at different temperatures (200–275 °C) were analyzed. Ni-based catalyst was the most active and selective catalyst towards CH_4 (80% CO_2 conversion at 250 °C, gas hourly space velocity (GHSV) = 509 $NmL\cdot(g_{cat}\cdot h)^{-1}$). The mechanism of CH_4 formation was proposed based on the observed intermediates, involving the formation of *CO and *HCOO species. This catalyst was then tested combined to zeolites 4A and 13 X. Under SEM conditions, the formation of hydrogen carbonate species was enhanced compared to conventional methanation, leading to a shift in product distribution toward CH_4. Zeolite 4A was the selected adsorbent since it was regenerated completely in multiple consecutive cycles unlike the zeolite 13X, which adsorbed a high amount of CO_2 which was not totally desorbed after the temperature swing process, and causing the generation of formates and carbonates during regeneration [69].

In 2024, Gómez et al. [70] scaled up the SEM process to a TRL 3 fixed bed reactor based on the results obtained in their previous works, namely using a zeolite 4A and a nickel-based catalyst. At 10 bar, during SEM stage at 230 °C, with a gas space velocity of 0.58 $kg\cdot(kg_{cat}\cdot h)^{-1}$ for a mixture of $H_2/CO/CO_2$, the best results were achieved with full conversion of CO, CO_2, and H_2 to SNG. To ensure the operability of the process, the absence of coke formation on the catalyst was verified. The optimal regeneration condition, performed over more than 10 reproducible adsorption/regeneration cycles with 100 vol% CH_4 during a pre-breakthrough time of 25 min, was found to be pressure swing to atmospheric pressure using a purge of 200 $NL\cdot h^{-1}$ of 10 vol% H_2/N_2 during 1 h. SEM was performed also at a higher gas space velocity (1 $kg\cdot(kg_{cat}\cdot h)^{-1}$) to improve the CH_4 productivity, fulfilling complete conversion and selectivity. A total of 5 reactors in parallel was estimated to be the optimal design to continuously carry out the process with 8 × 10^{-4} $mol_{CH_4}\cdot(kg_{cat}\cdot s)^{-1}$ productivity [70]. Finally, the same authors, in the TRL 3 fixed bed reactor, with the parameters set by the previous analysis (pressure of 10 bar and Ni-based catalyst and zeolite 4A), assessed the effect of temperature and inlet gas composition considering H_2/CO_2 or $H_2/CO_2/CO$ mixtures and a synthetic syngas, corresponding to the composition of a gas from SEG of wood with CaO as bed material. Temperatures and gas space velocities ranged between 200 and 230 °C and between 0.8 and 1.4 $kg_C\cdot(kg_{cat}\cdot h)^{-1}$, respectively. 87% of CH_4 in the product gas was achieved for CO_2 SEM, while the purity reached 100% using $H_2/CO/CO_2$ mixtures since in this case less CO_2 was adsorbed on zeolite. When the reactor was fed with synthetic syngas, a H_2 feed above the stoichiometric was necessary for converting the hydrocarbons considered in the mixture (C_2H_4, C_2H_6, C_3H_6), achieving pure CH_4 for 30 min at a space velocity of 0.8 $kg_C\cdot(kg_{cat}\cdot h)^{-1}$ and for 16 min at almost double space velocity conditions (i.e., 1.4 $kg_C\cdot(kg_{cat}\cdot h)^{-1}$). The study confirmed the potential of the SEM process using both biomass derived syngas and renewable H_2 and CO_2, highlighting the importance of optimizing the effect of the involved variables to allow the reproducibility on a large-scale SNG process [71].

Turning again to SEM applied to biogas upgrading, an experimental work was published recently by Mercader et al. [72]. They used a catalyst with 7.5/2.5 $wt\cdot wt^{-1}$ Ni–Fe supported on γ-Al_2O_3 and zeolite 5A as the sorbent in a fixed bed reactor. A first set of experiments involved pure CO_2 hydrogenation with a stoichiometric gas supply, and then a typical sweetened biogas stream (molar ratio CH_4/CO_2 = 7/3) was considered. The Fe–Ni catalyst demonstrated stability throughout the experimental cycles and 5A zeolite proved to enhance CO_2 hydrogenation with a CO_2 conversion increased during the first methanation cycle by more than 20%

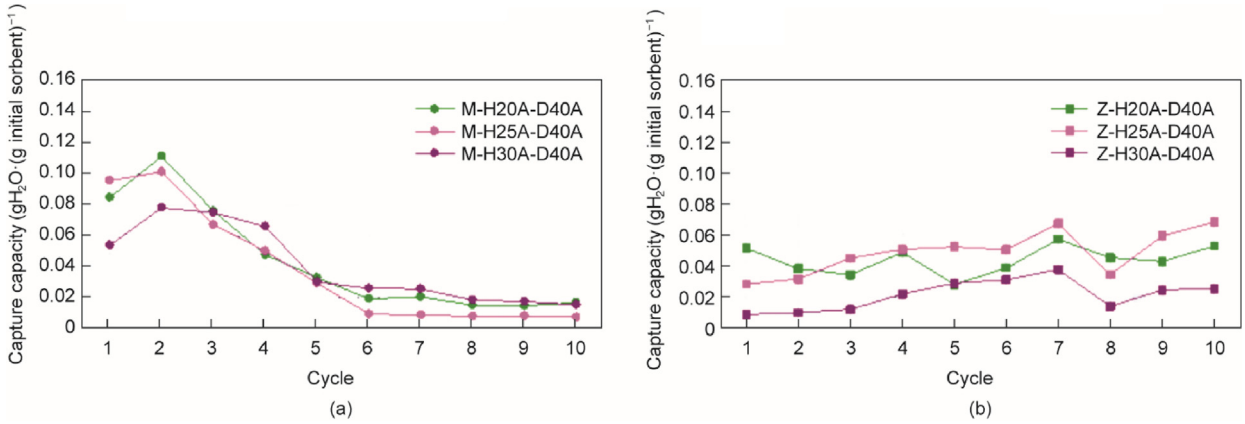

Fig. 15. H_2O capture capacity over the cycles for (a) calcium oxide and (b) zeolite 3A at hydration temperatures of 200, 250 and 300 °C and dehydration temperature of 400 °C. Reproduced from Ref. [65] with permission.

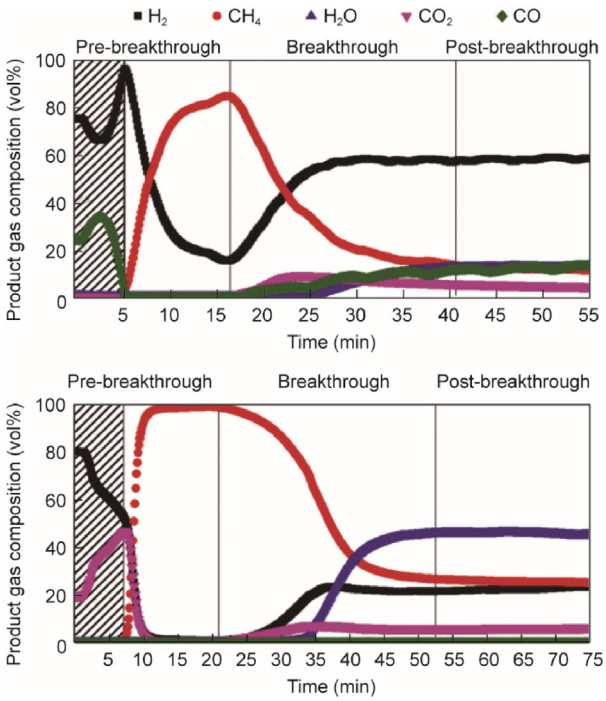

Fig. 16. Outlet gas concentration during SEM at 275 °C: CO SEM (top) and CO_2 SEM (bottom). Space velocity for CO and CO_2 was kept at 0.58 $kg\cdot(kg_{cat}\cdot h)^{-1}$ corresponding to 440 $mL_{CO}\cdot(g_{cat}\cdot h)^{-1}$ for CO SEM and 300 $mL_{CO_2}\cdot(g_{cat}\cdot h)^{-1}$ for CO_2 SEM. Reproduced from Ref. [67] with permission.

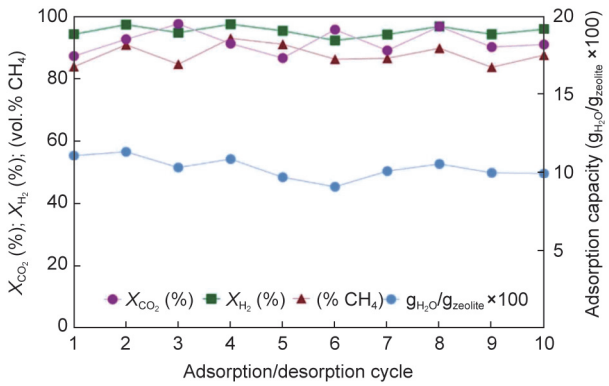

Fig. 17. H_2O adsorption capacity, X_{CO_2}, X_{H_2}, and CH_4 content during the pre-breakthrough over 10 SEM/regeneration cycles at 275 °C with a gas space velocity of 230 $NmL\cdot(g_{cat}\cdot h)^{-1}$. Reproduced from Ref. [68] with permission.

compared to the condition without zeolite. This intensification reduced after the first cycle, and it was only recovered after a desorption step rising the temperature up to 500 °C. It was found that around 350 °C, the negative effect of CH_4 in the feed on the conversion was minimal, being at this temperature the selectivity to CO very low.

2.5. Modeling of SEM

From the perspective of reactor design and up-scaling, Kiefer et al. [73] coupled an experimental and modeling analysis to give a comprehensive overview of the mechanisms dominating the process in a fixed bed. The dynamic behavior of the coupled water adsorption and reaction front is strictly linked to the heat generation in the reactor, which remains a major challenge for process performance and product purity. The interplay between thermal behavior, adsorption and the resulting performance of a fixed bed with pelletized nickel-impregnated zeolite 13X was investigated, giving a guide for reaction engineering. The constraints represented by the zeolite sorption isotherm, hydrothermal stability, and transport properties, also considering the interaction with the catalyst and its properties, the residence time and the heat removal, are the aspects to be considered for the correct design of the process, which results closer to a zeolite-based gas drier reactor than to a conventional catalyst reactor. The work was continued by Barbaresi et al. [74], who developed a model of a fixed bed SEM system, further validated with experimental data, that describes the dynamic behavior during methanation and sorbent regeneration with alternating operation of two reactors for continuous production. The model was able to predict the species concentrations, the temperature front, and the bed regeneration dynamics, confirming the results of experiments in the literature that showed complete CO_2 conversion. The saturation degree, defined as the ratio of retained water to the saturation value, was identified as the key parameter: As the saturation degree increases, the improvement in reaction performance due to water removal diminishes, along with the conversion. Cañada-Barcala et al. [75] coupled an experimental campaign to obtain the kinetic parameters of a commercial Ni/SiAl catalyst to the simulation of methane production in a cyclic fixed bed sorption-enhanced reaction process using the parameters experimentally obtained and considering zeolite 3A as the water selective adsorbent. Three

consecutive stages were considered for the process: an adsorption/methanation stage, followed by rinse and purge, to desorb the adsorbed water and remove it by condensation, with the aim of obtaining an effluent suitable for domestic natural gas usage. The selective adsorption of water by the commercial Ni/SiAl catalyst was verified and eventually the Xu and Froment's model [43] was used to predict the experimental data from the kinetic characterization in the fixed bed. The process was then simulated obtaining a stream fulfilling the domestic natural gas standards with a CO_2 conversion of 99.73%, a CH_4 selectivity of 99.99% and a compression energy consumption (6.97 $kJ{\cdot}mol^{-1}$ CH_4) 99 times lower than the heat of combustion of methane. The same authors designed a biogas upgrading process investigating two different catalysts, $NiAl_2O_3$ and Ni5A, as compared with a commercial catalyst (Ni/SiAl), in an experimental fixed bed in the range 473–623 K. The Ni5A catalyst showed lower reaction yields and was thus excluded from the subsequent simulations, based on a theoretical model of reaction/adsorption cycles designed using zeolite 3A as the adsorbent, and involving the experimental kinetic data. With the primary aim of producing SNG suitable for the gas grid specifications, by studying as variables the temperature and the composition of the biogas feed, the operating conditions were optimized at 488 K for a residual waste biogas composition of 55%–60% CH_4 at atmospheric pressure, under which CO_2 conversion of 99.55%, selectivity of 99.99%, and methane purity in the product of 98.6% were achieved using a $NiAl_2O_3$-zeolite 3A mixture, selected for its high yield at low temperatures [76].

The target generally found in the literature (i.e. to produce methane streams suitable for injection into the natural gas grid), was also set in the simulation works by Coppola et al. [77] and Massa et al. [78], which modeled in Aspen Plus, by means of the FluidBed reactor block, a chemical looping scheme proposed to perform SEM, based on dual interconnected fluidized beds. Low-cost CaO derived from limestone as sorbent for steam capture and a traditional Ni-based catalyst were applied in these studies. In the first work, they considered a feeding gas consisting of a mixture of H_2, CO_2, and CO, investigating the optimal operating conditions in terms of feeding gas composition, recirculation of CaO between the two reactors and methanation temperature in the range 250–350 °C. The aim was to optimize the SEM process using cheap CaO, despite the detrimental effect due to the unwanted parallel carbonation reaction. The results showed that the negative impact on methanation of CaO carbonation reaction when a stoichiometric gas feeding was fed into the methanator, causing an increase of H_2 concentration, led to an outlet gas unsuitable for direct injection in the gas grid, with the only exception at 250 °C for pure CO methanation. Conversely, under H_2 sub-stoichiometric feeding gas, optimal conditions could be individuated as a function of the methanation temperature, with the surplus of fed CO_x compensated by the effect of CaO carbonation. However, at the highest methanation temperature of 350 °C, again no conditions could be detected for a proper outlet gas quality. The identified conditions may be of interest for H_2-lean gas such as syngas from gasification. A parallel thermodynamic analysis in this study highlighted the possible carbon formation induced by SEM conditions coupled to H_2 sub-stoichiometric feeding. However, the simultaneous capture of H_2O and CO_2 by CaO may affect the system positively in this respect, due to the limited carbon enrichment in the reaction environment [77]. In addition to the syngas-type feedings, Massa et al. [78] simulated biogas upgrading via the same process and configuration. Again, with a stoichiometric ratio of the gas feeding, no conditions could fulfill the grid specifications even at the lowest temperature of 250 °C. On the contrary, for H_2-lean feedings, at 300 °C conditions could be found to ensure a product quality matching the grid specifications for both CH_4-lean and CH_4-rich biogas.

Bareschino et al. [79] modelled SEM with a Ni on zeolite 13X bi-functional pellet in a two-dimensional, heterogeneous, externally cooled fixed bed reactor. The sensitivity analysis concerned the effects of GHSV and pressure on methane purity and effective operational time. Good agreement was found by validating the mathematical model with experimental data from the literature. The temperatures inside the reactor showed a non-uniform distribution, with gradients of about 100 °C, leading to an uneven distribution of adsorbed water. Being the reaction rate limiting, a faster convective mass transfer could lead to reactants slip resulting in breakthrough times lower than the water one. However, pure and dry methane flow could be obtained in the pre-breakthrough period. A non-monotonic negative correlation between GHSV and breakthrough times existed, while the increase in operating pressure always led to an increase of breakthrough time, the prediction of which was fundamental to optimize or intensify the process, in terms of number of parallel reactors and co-occurrence of the different steps. Even a moderate increase in operating pressure (for typical GHSV values reported in the literature of 2–2.5 $m^3{\cdot}\ (kg_{ads}{\cdot}h)^{-1}$), made the water breakthrough times exceed the one corresponding to atmospheric pressure. Overall, the authors highlighted promising perspectives for this technology, the results showing how the optimization of the operating conditions can allow for quite long-time intervals during which high-purity methane is attained, even at low pressures. The same group modelled the process in an adiabatic packed bed, with a five-stage sequence describing SEM and subsequent solid regeneration, consisting in methanation/water removal, and then drying by pressure and temperature swing approach (blowdown, purge, cooling, and pressurization). The effect of gas inlet temperature, pressure, and GHSV on system performance was assessed. While in adiabatic operation temperature control was complex, the produced heat may be efficiently used for the drying stage. The study showed that the gas feeding temperature should not exceed 260 °C to prevent harmful temperatures. The heat generated during the SEM phase was sufficient to regenerate the solid at pressure values of 4 and 8 bar. However, when compared to isothermal or cooled reactors, the configuration investigated offered lower purity levels due to the high temperatures limiting the sorbent adsorption capacity. Continuous methane production was achieved by operating three reactors in parallel with an appropriate regeneration phase, with a purity over 98% for pressures greater than 2 bar [80].

In a concluding view, as anticipated before, SEM studies are still focused on the development of better performing materials and reactor configurations, and in terms of technology development, applications for optimization, scaling up and processes integration are still lacking. In this direction, in order to propose an integrated layout to realize the SEM process within the CCU technologies, Chirone et al. [81] investigated, in terms of technical, economic, and environmental issues, a novel plant layout involving catalytic methanation for the production of renewable SNG, combined to calcium looping for CO_2 capture from flue gases of a coal-fired power plant and proton exchange membrane (PEM) water electrolysis for the production of green H_2. The techno economic and life cycle assessment (LCA) performances were compared with those of traditional natural gas production and biomethane production from maize silage. They showed how the production cost of synthetic methane per unit Nm^3, although clearly still higher than that of natural gas, may be lower than that of bio-methane. The PEM electrolyzer, particularly for electricity consumption, accounted for most of both costs and environmental impacts of the process. It is worth mentioning however, that PEM costs are forecasted by many studies to significantly decrease in the coming years. The LCA analysis showed no systems outperforming the others over all categories, and from a climate change perspective many issues remain to be optimized so that the proposed layout may be

effectively advantageous when compared to the conventional pathway for methane production.

3. Sorption-enhanced hydrogenation to MeOH, DME, and SERWGS

Unlike SEM, there are relatively fewer publications on the equivalent processes to produce MeOH, DME, and CO (via the RWGS reaction). However, interest in these processes—both scientific and industrial—is steadily increasing, particularly within the context of the energy transition. A list of relevant studies available in the literature is presented in Table 2 [87–105]. Despite the limited number of publications, a detailed review of the main findings is provided below.

3.1. Sorption-enhanced hydrogenation of CO_2 to MeOH

3.1.1. Catalytic hydrogenation to MeOH overview

MeOH has a long history that dates back to ancient Egypt, and the evolution of its synthesis process is well documented in Sheldon's work [82]. Today, MeOH ranks among the top five most produced chemicals, serving as a key feedstock to produce olefins—intermediates used to manufacture hundreds of products, including formaldehyde, acetic acid, and methyl tert-butyl ether (MTBE), which are essential components in paints, plastics, and resins. Commercial MeOH is primarily produced from syngas derived via steam reforming of methane, typically under conditions of 250–300 °C and 50–100 bar, using $Cu/ZnO/Al_2O_3$ (CZA) catalyst, and various reactor configurations [30].

MeOH production could be significantly expanded by coupling green hydrogen with CO_2 capture and utilization process, thereby promoting its broader use in the production of fuels and chemicals. This aligns with the concept of a MeOH economy, originally proposed by Olah and colleagues [83–85]. A notable example of this sustainable approach is the carbon recycling international plant in Iceland, which produces 5 million liters of MeOH annually. In this facility, hydrogen is generated through water electrolysis powered by renewable energy sources—primarily geothermal, hydro, and wind [86].

The main reactions that take place during catalytic MeOH production are the CO_2 hydrogenation to MeOH (Eq. (4)) and the RWGS reaction (Eq. (3)):

$$CO_2 + 3H_2 \rightleftarrows CH_3OH + H_2O,\ \Delta H_{298K} = -49.4\ kJ\cdot mol^{-1} \quad (4)$$

$$CO + 2H_2 \rightleftarrows CH_3OH,\ \Delta H_{298K} = -90.5\ kJ\cdot mol^{-1} \quad (5)$$

Furthermore, hydrogenation of CO to MeOH is possible, although to a lesser extent.

From a thermodynamic point of view, low temperatures and high pressures are ideal for MeOH production, at 440 bar of pressure MeOH selectivity reaching 95%. Concerning the possible catalysts for this process, a summary of the vast literature on the topic can be found in the review of Álvarez et al. [30].

3.1.2. Thermodynamics of sorption-enhanced hydrogenation to MeOH

For MeOH production, the sorption-enhanced process is proposed for essentially the same reasons as for methanation: to improve performance at lower pressures and moderate temperatures by overcoming thermodynamic limitations. One of the most comprehensive studies on the thermodynamic aspects of SEMeOHS was conducted by Zachopoulos and Heracleous [87]. In their work, various operating parameters—such as temperature, pressure, the H_2/CO_2 feed ratio, and the sorbent's sorption capacity (defined as the molar uptake of H_2O relative to the stoichiometric amount of H_2O produced by Eqs. (3) and (4) at full conversion)—were systematically varied to identify optimal conditions. The study highlights both the advantages and limitations of the sorption-enhanced process in comparison to conventional synthesis without sorbents. The analysis was conducted by modeling both processes in Aspen Plus, using an RGibbs reactor (i.e., assuming thermodynamic equilibrium) for MeOH production.

The study was based on several simplifying assumptions: Only Eqs. (3) and (4) were considered, and the sorbent was assumed to selectively adsorb only water, excluding other compounds such as MeOH. Under conventional (non-sorption-enhanced) conditions—indicated in orange in Figs. 18(a) and (b) [87]—an increase in temperature (within the range of 100 to 350 °C) had a detrimental effect on MeOH selectivity, yield, and CO_2 conversion, which reached a minimum around 270 °C. This trend can be explained by the thermodynamics of the reactions involved: Increasing temperature negatively affects the exothermic CO_2 hydrogenation reaction while promoting the endothermic RWGS reaction. This is further supported by the observation that CO_2 conversion closely matches CH_3OH yield at lower temperatures but begins to diverge at higher temperatures, where CO formation becomes dominant, as reflected in the drop in MeOH selectivity.

Thermodynamics would suggest operating at the lowest possible temperature to maximize conversion. However, reaction kinetics may be too slow under such low temperatures, rendering the process impractical. Notably, as the authors point out, even at 100 °C, the maximum achievable conversion remains below 80%. In contrast, practical reaction rates—achievable with commercial catalysts—occur between 220 and 270 °C, resulting in CO_2 conversions below 35% and CH_3OH yields of around 50%.

The introduction of a water sorbent into the system (Figs. 18(a) and (b), blue lines) results in a substantial increase in CO_2 conversion—reaching nearly 100% across the entire temperature range analyzed—with only negligible water vapor present in the outlet stream. MeOH yield also shows a significant improvement, with increases of up to 130% in the temperature range of practical interest (220–270 °C). However, MeOH selectivity experiences a slight decrease compared to conventional conditions, as the sorption-enhanced effect also promotes the RWGS reaction, leading to increased CO production.

Figs. 18(c) and (d) illustrate the effect of pressure, ranging from 1 to 100 bar, on both the traditional process (orange lines) and the sorption-enhanced process (blue lines). Under conventional conditions, increasing pressure has an overall positive effect on all process variables. Specifically, higher pressure favors MeOH synthesis, while the RWGS reaction remains largely unaffected. Transitioning to sorption-enhanced conditions leads to complete CO_2 conversion and a significant increase in MeOH yield. The removal of water from the reaction system also results in a dry outlet gas stream. In this scenario as well, MeOH selectivity is the only parameter negatively impacted by the sorption-enhanced process.

An increase in the H_2/CO_2 molar feed ratio positively impacts process performance under both traditional and sorption-enhanced conditions (Figs. 18(e) and (f)). In conventional conditions, both CO_2 conversion and MeOH yield increase as the feed ratio rises. From a thermodynamic perspective, a higher H_2/CO_2 ratio favors the MeOH synthesis reaction over CO formation, as evidenced by the corresponding increase in MeOH selectivity. Even in the presence of the sorbent, increasing the H_2/CO_2 ratio has a positive effect, leading to overall improvements in process performance in terms of CO_2 conversion and MeOH yield. However, for H_2/CO_2 ratios below 1.5—close to the stoichiometric value for the RWGS reaction—the system exhibits a lower MeOH yield compared to traditional conditions. In this range, both MeOH yield and selectivity drop to zero.

Table 2
Main studies on sorption-enhanced hydrogenation to MeOH, DME, and SERWGS.

Catalyst/sorbent	Reactor type	Feed comp. ($\%_{vol}$) H_2/CO_2+CO/inert	SE Temp. (°C)	Regen. Temp. (°C)	Press. (bar)	GHSV	Sample mass (g)	H_2O upt. ($mmol \cdot g^{-1}$)	Max. conversion	Max. selectivity	Refs.
SEMeOHS studies											
CZA/zeolite 4° (mixed)	Fixed bed (simulation)	50–83.3/16.7–50/0	100–350	100–350	1–100	N.A.	N.A.	15.8	99.9 (CO_2), 80.6 (H_2)	~100% (MeOH)	[87]
CZA/zeolite 3A (mixed)	Fixed bed (experimental)	68.2/22.7/9.1	210–270	230	20–60	2 800–5 600 h^{-1}	N.A.	N.A.	~30% (CO_2)	~45% (MeOH)	[88]
CZA/zeolite 3A (mixed)	Fixed bed (experimental)	73.5/24.5/2	200–300	200–300	50	N.A.	0.85–1.84 (cat.) + 7.36–7.65 (sorb.)	N.A.	83.6 (CO_2)	79.6% (MeOH)	[89]
CZA/zeolite 13X (mixed)	Fixed bed (experimental)	75/25/0	225–275	275–300	70	12 000 $mL \cdot (g_{cat} \cdot h)^{-1}$	N.A.	N.A.	~45% (CO_2)	~80% (MeOH)	[90]
CZA/zeolite 3A (mixed), CZA/silica gel (mixed), CZA/silica-alumina (mixed)	Fixed bed (simulation)	N.A.	250	250	50	N.A.	N.A.	N.A.	42.3 (CO_2)	70.9% (MeOH)	[91]
CZA/zeolite 3A & 4A & 5A & 13X (mixed)	Fixed bed (experimental)	75/25/0	250	300	70	12 000 $mL \cdot (g_{cat} \cdot h)^{-1}$	0.5 (cat.) + 4.0 (sorb.)	0.3–1.6	~40% (CO_2)	~72% (MeOH)	[92]
Cu/zeolite 13X (bi-functional)	Thermo-balance (experimental)	86/14/0	200–300	400	15	N.A.	2	N.A.	N.A.	~35% (MeOH)	[93–95]
CZA/zeolite 3A (mixed)	Fixed bed (simulation)	75/25/0	210–270	210–270	50	200–800 h^{-1}	N.A.	N.A.	N.A.	N.A.	[96,97]
SEDMES studies											
CZA-HZSM-5/zeolite 4A (mixed)	Fixed bed (simulation)	50–66.7/33.3–50/0	250	N.A.	50	N.A.	N.A.	N.A.	~95% (H_2)	~99% (DME)	[98]
CZA-γAl_2O_3/zeolite 3A (mixed)	Fixed bed (simulation)	72.7/27.3/0	225–300	400	10–50	320–1 280 $mL \cdot (g_{ads} \cdot h)^{-1}$	N.A.	N.A.	> 80% (CO_2)	~85% (DME)	[99]
CZA:PTA-γAl_2O_3/zeolite 3A (mixed)	Fixed bed (experimental)	60/20/20	225	225	30	1 750 h^{-1}	1 (cat.) + 1–12 (sorb.)	N.A.	~80% (CO_2)	N.A.	[100]
CZA-γAl_2O_3/zeolite 3A (mixed)	Fixed bed (experimental)	68.6–72.7/17.1–32.7/balance	200–300	200–400	5–30	92–153 h^{-1}	0.5 (cat.) + 5.0 (sorb.)	N.A.	~80% (CO_2)	~80% (DME)	[101,102]
SERWGS studies											
Pt/zeolite 4A & 13X (bi-functional), Cu/zeolite 4A & 13X (bi-functional)	Fixed bed (experimental)	40/10/40	300–325	400	1–29	120–276 $mL \cdot (g_{ads} \cdot h)^{-1}$	8.7–25	0.83–1.62	95% (CO_2)	~100% (CO)	[103]
Cu-UGSO/zeolite 13X (mixed)	Fixed bed (experimental)	52.5/17.5/30	200–300	400	1	4800 $mL \cdot (g_{ads} \cdot h)^{-1}$	0.5 (cat.) + 0.5–2 (sorb.)	2–4	30.9% (CO_2)	~100% (CO)	[104]
Cu/zeolite 13X (mixed)	Fixed bed (simulation)	52.5/17.5/30	225–300	N.A.	1	4800 $mL \cdot (g_{ads} \cdot h)^{-1}$	0.5 (cat.) + 2 (sorb.)	2–4	N.A.	N.A.	[105]

Finally, the sensitivity analysis on sorbent capacity shows that a value close to 1 is sufficient to maximize MeOH yield, while higher capacities offer no additional benefit.

Overall, from a thermodynamic standpoint, the process benefits from sorption-enhanced conditions in terms of both CO_2 conversion and yield of the desired product (CH_3OH). However, MeOH selectivity is negatively affected, as water adsorption also promotes the RWGS reaction. It is important to highlight that the high reagent conversion and the ability to obtain a dry product represent significant advantages in terms of process design. These factors can potentially simplify the plant configuration by reducing the need for recycling unconverted reactants and easing the separation and purification steps for the final product.

3.1.3. Experimental studies of sorption-enhanced hydrogenation to MeOH

The results of the thermodynamic analysis were confirmed by several experimental studies conducted in fixed bed reactors by different research groups. For example, in the work of Maksimov et al. [88], it was clearly demonstrated that sorption-enhanced conditions—using commercial CZA catalyst and a 3A molecular sieve as the sorbent—led to a significant increase in the conversion of both CO_2 and H_2 compared to the traditional process. However, in terms of selectivity, CO formation was more strongly favored than CH_3OH, with CO output increasing by 220%–510%, compared to 150%–290% for MeOH. Additionally, increasing the pressure, particularly above 40 bar, was shown to improve selectivity toward the desired product. The optimal reaction temperature was found to be around 250 °C, representing the best compromise between kinetics and thermodynamics—favoring CO_2 hydrogenation over the RWGS reaction. Similar findings were reported by Pascual-Muñoz et al. [89], who also used a commercial catalyst and a 3A molecular sieve. In their study, an optimal catalyst-to-sorbent mass ratio of 20:80 was identified, noting that higher sorbent loadings did not further improve CO_2 conversion or MeOH selectivity.

The use of a 13X zeolite as a sorbent, as proposed by Heracleous et al. [90], showed a positive effect under sorption-enhanced conditions, with trends consistent with the thermodynamic expectations of the process. Notably, MeOH yield increased by approximately 115% at 225 °C. However, a decrease in MeOH selectivity compared to traditional conditions was also observed, confirming the competitive nature of CO_2 hydrogenation and the RWGS reaction. The same authors, in a detailed investigation of the cyclic MeOH production/adsorption-regeneration process, found that MeOH was also adsorbed on the sorbent along with

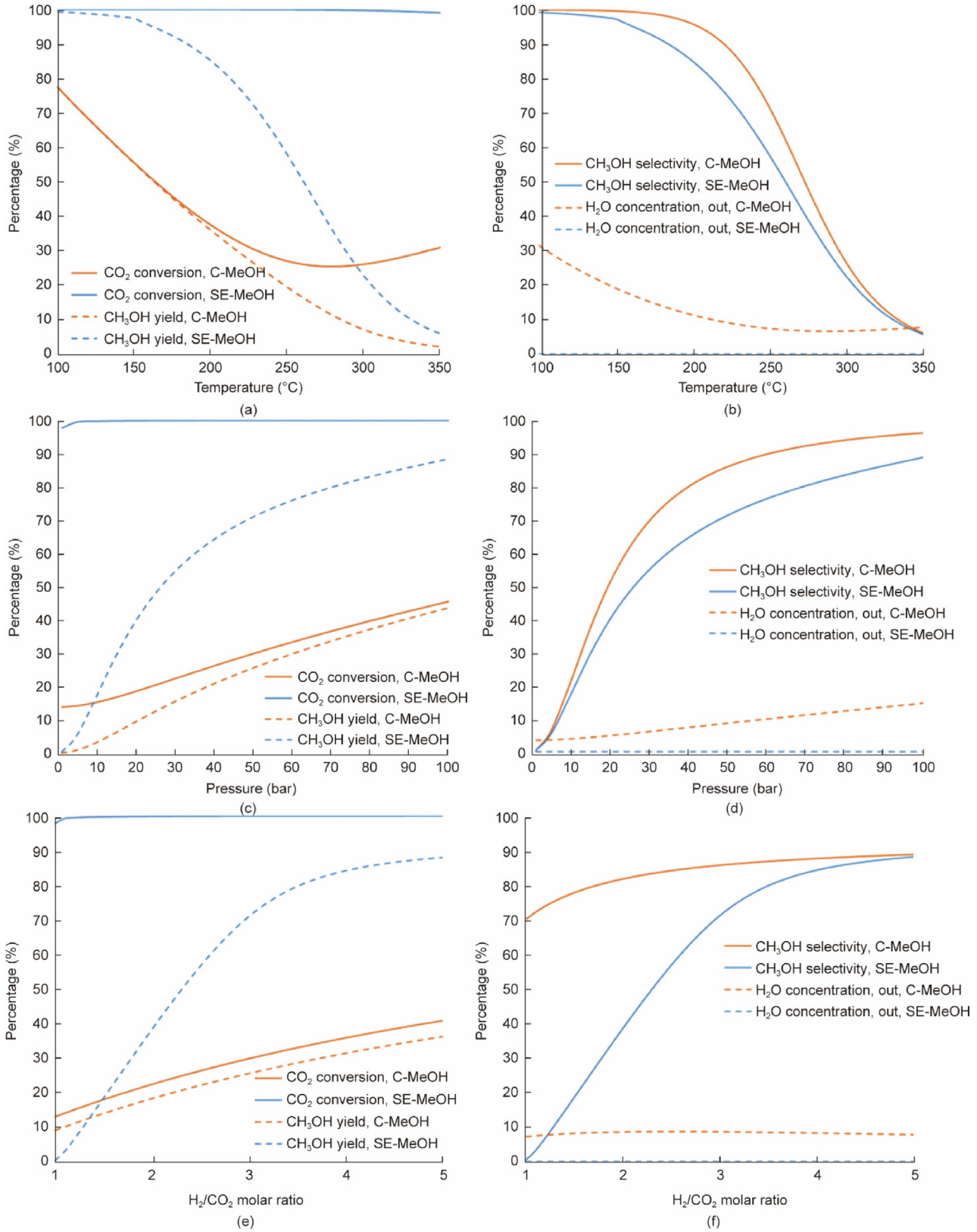

Fig. 18. CO_2 conversion, CH_3OH yield, CH_3OH selectivity, and H_2O outlet concentration for the conventional and the SEMeOHS processes. (a, b) Effect of temperature at P = 50 bar, H_2/CO_2 ratio = 3; (c, d) effect of pressure at T = 230 °C, H_2/CO_2 ratio = 3; (e, f) effect of H_2/CO_2 molar ratio in the feed at T = 230 °C, P = 50 bar. Reproduced from Ref. [87] with permission.

water vapor. Analysis of the desorbed liquid during regeneration revealed MeOH concentrations in the range of approximately 26%–43% by weight.

All sorption-enhanced processes share the common challenge of identifying the optimal sorbent that meets the process requirements. The catalytic synthesis of MeOH is no exception, with

zeolites being the primary candidates for this role. However, unlike methanation, the SEMeOHS faces an additional complexity due to competitive adsorption between water and MeOH on the zeolite sorbents. This specific issue has been the focus of investigation by several research groups.

In a recent study, Heracleous et al. [92] investigated four zeolites (3A, 4A, 5A, and 13X) as potential water sorbents in mechanical mixtures with a commercial CZA catalyst, using a thermogravimetry-mass spectrometry (TG-MS) apparatus. Adsorption and desorption tests were performed with water, MeOH, and water–MeOH mixtures. The results showed that water sorption capacity decreased significantly with increasing temperature but remained substantial even at 250 °C, which is relevant for typical MeOH synthesis conditions from CO_2. Generally, zeolites with larger pore sizes (13X and 5A) exhibited higher sorption capacities and faster adsorption kinetics, but required higher desorption temperatures due to stronger adsorbent–adsorbate interactions. For MeOH, sorption kinetics were significantly faster than for water, and sorption capacities were notably higher, with more pronounced differences among the zeolites. Like for water, the zeolites with larger pores demonstrated the highest MeOH uptake. Under conditions with both water and MeOH present, tests revealed that 3A and 5A zeolites had many sites favoring preferential MeOH adsorption, whereas 4A and 13X zeolites exhibited numerous sites for competitive adsorption of both compounds. Ultimately, zeolites 4A and 13X led to slightly higher activity enhancements compared to 3A and 5A, as illustrated in Fig. 19 [92].

Although the simultaneous adsorption of both water and MeOH might be viewed as a drawback in the use of zeolites, it enables a preferential enhancement of CH_3OH production over CO due to a stronger thermodynamic equilibrium shift favoring MeOH synthesis. In fact, zeolite 5A—which exhibited the highest MeOH uptake—also achieved the greatest improvement in MeOH selectivity.

Sorbent stability tests under cyclic operation showed that deactivation was primarily caused by incomplete desorption of water and MeOH at the regeneration temperature of 300 °C, along with possible alterations in the sorbents' structural and textural properties under reaction conditions. Among the zeolites tested, 13X exhibited the highest deactivation, followed by 5A and 3A, while zeolite 4A demonstrated the greatest stability.

Pasqual-Muñoz et al. [91] also tested various materials as potential sorbents for MeOH synthesis, including silica gel and silica-alumina, comparing them to 3A zeolite. While 3A zeolite demonstrated the best performance with higher MeOH productivity—attributed to its greater affinity for water compared to silica-alumina and silica gel—it is important to note that MeOH was not adsorbed on silica gel at high temperatures (> 200 °C). In contrast, MeOH adsorption was stronger on silica-alumina than on 3A zeolite.

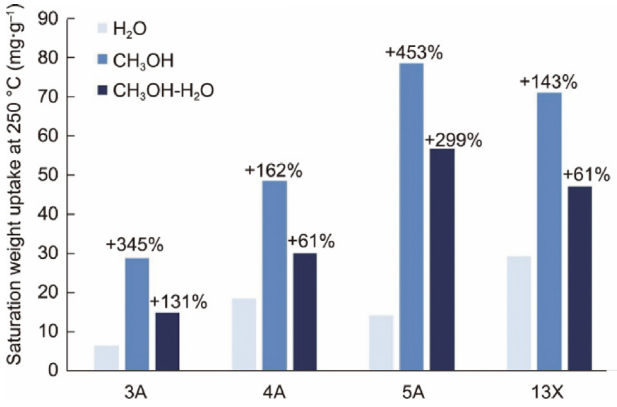

Fig. 19. Total uptake for zeolites 3A, 4A, 5A, and 13X of H_2O, CH_3OH, and CH_3OH-H_2O at 250 °C. The values correspond to the relative increase in mass compared to adsorption of pure H_2O only. Reproduced from Ref. [92] with permission.

The potential to chemically modify zeolites to enhance their performance in the process was the primary focus of a study by Pascual-Muñoz et al. [94]. Specifically, they investigated how varying the proportions of sodium and potassium in the zeolites affected the adsorption of MeOH and water. On sodium-exchanged zeolites, MeOH was adsorbed more strongly than water at 200 °C; however, this trend reversed at higher temperatures, with water exhibiting greater affinity than MeOH (Fig. 20 [94]).

The substitution of sodium with potassium increased the zeolite's affinity for water, as the larger potassium ions hinder MeOH diffusion within the pores, thereby limiting its access to adsorption sites. These findings align with those reported by Terreni et al. [93], which demonstrated that selectivity can be influenced by variations in temperature.

3.1.4. Modeling of sorption-enhanced hydrogenation to MeOH for reactor optimization

Maksimov et al. [97] investigated the optimization of a plant operating under sorption-enhanced conditions by developing a mathematical model to identify the best operating parameters, based on the flowsheet shown in Fig. 21. The study primarily focused on determining the optimal reactor temperature and catalyst-to-adsorbent ratio to produce a MeOH stream with controlled water content. Among the variables examined, both quasi-isothermal and adiabatic reactor configurations were evaluated, with and without the inclusion of a guard sorbent layer—a layer placed at the reactor outlet to enhance the purity of the main product.

The results indicated that the specific MeOH production rate was strongly influenced by the GHSV, reflecting that sorption-enhanced synthesis is constrained by the low flow rates needed to effectively remove water. The optimal reactor temperature was identified as approximately 215 °C for the adiabatic reactor and 235 °C for the quasi-isothermal reactor. The ideal catalyst mass fractions were about 0.65 for the adiabatic reactor and 0.50 for the quasi-isothermal reactor. Overall, the quasi-isothermal reactor equipped with a guard adsorbent layer emerged as the best configuration, capable of producing MeOH with a purity of 99 wt%.

Conversely, from a techno-economic perspective, the same research group found that the adiabatic configuration is more competitive due to the higher capital costs associated with the quasi-isothermal setup [96]. Although the sorption-enhanced process entails higher capital expenses than the conventional process—mainly because it requires a multi-reactor system to handle production and regeneration cycles, as well as increased reactor volume to accommodate the sorbent—these costs are balanced by reduced operating expenses thanks to more efficient hydrogen utilization. The overall production cost for the adiabatic sorption-enhanced process was found to be comparable to that of the conventional process. Further improvements were anticipated through optimization of cycle design and timing, reactor configuration, and the overall process design, including product separation. Regarding this last aspect, the study proposed an SEMeOHS process aiming to produce purified MeOH without distillation at the reactor outlet; however, as the authors noted, the separation and purification scheme could be tailored and optimized based on the purity of the crude MeOH.

3.2. Sorption-enhanced hydrogenation of CO_2 to DME

Although MeOH is considered a good fuel for fuel cells and an excellent blend component for internal combustion engines, its low cetane number—around 3—prevents its direct use as the sole

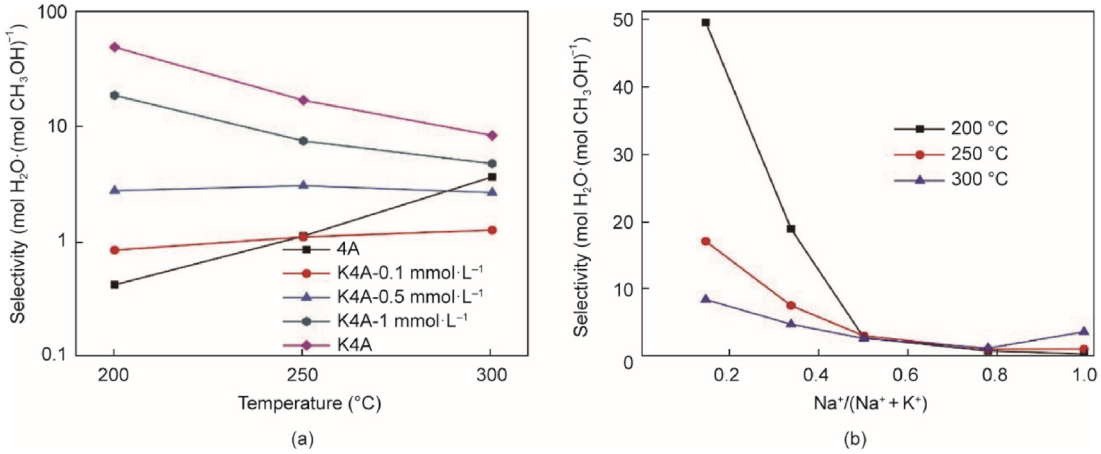

Fig. 20. Water/MeOH selectivity for all the adsorbents calculated as a function of (a) temperature and (b) sodium proportion. Reproduced from Ref. [94] with permission.

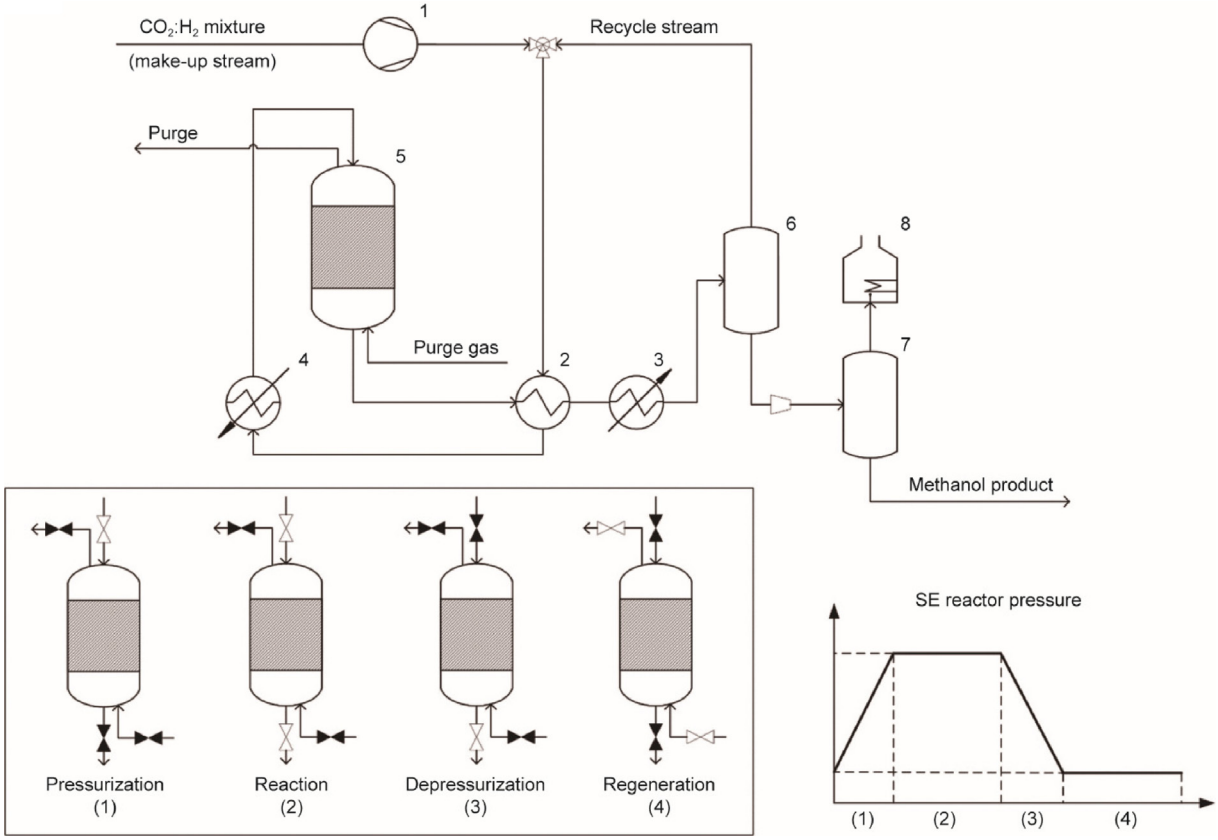

Fig. 21. Flowsheet of the SEMeOHS process. 1: compressor; 2: heat exchanger; 3: cooler; 4: heater; 5: SE reactor; 6: high pressure flash drum; 7: low pressure flash drum; 8: purge gas combustor. Reproduced from Ref. [97] with permission.

fuel in diesel engines. In contrast, DME has a high cetane number, typically between 55 and 60, comparable to conventional diesel fuels (which range from 40 to 55). Additionally, DME produces significantly lower emissions of particulate matter, NO_x, and CO compared to traditional fuels, and it boasts excellent biodegradability.

DME is produced through the dehydration of MeOH using an acidic catalyst, following the reaction below, and typically under the same temperature and pressure conditions as MeOH synthesis:

$$2CH_3OH \rightleftarrows CH_3OCH_3 + H_2O,\ \Delta H_{298K} = -23.4\,kJ\cdot mol^{-1} \quad (6)$$

Typical catalysts for dehydration of MeOH include γ-Al_2O_3 and H-ZSM-5: γ-Al_2O_3 is the most widely used catalyst industrially due to its good acidity and high surface area; however, its activity is inhibited by the presence of water, primarily because water competes with MeOH for the active sites [106]. In contrast, H-ZSM-5 possesses both Lewis acid sites and a higher number of stronger Brønsted acid sites compared to γ-Al_2O_3 resulting in higher activity and excellent resistance to water inhibition [107]. A more detailed and comprehensive discussion on catalysts for DME synthesis is available elsewhere [30].

Beyond its use as a fuel, DME serves as a valuable feedstock for producing olefins and aromatics, and as a hydrogen carrier due to its ease of liquefaction and storage [108]. Its production becomes even more attractive within the context of the energy transition, especially when integrated with CO_2 capture and green hydrogen production.

Commercially, DME is produced from syngas (CO, CO_2, and H_2) via a two-step process: first, MeOH is synthesized from syngas using the conventional CZA catalyst; then, MeOH undergoes dehydration over an acidic γ-Al_2O_3 catalyst [109]. This sequential configuration faces thermodynamic limitations, resulting in a limited DME yield and necessitating extensive separation and significant recycling of unreacted feedstocks.

Potential improvements could be achieved through a one-step process that combines both the MeOH synthesis catalyst and the MeOH dehydration catalyst within the same reactor, either by mixing them or by depositing both active phases on a single support to create a hybrid catalyst [110,111]. This approach would reduce the number of process steps and, from a thermodynamic perspective, shift the equilibrium toward MeOH production by continuously consuming MeOH *in situ* via dehydration to DME, thereby increasing the overall DME yield. Thermodynamic studies have shown that the equilibrium conversion of CO_2 to DME is significantly higher than that for CO_2 to MeOH alone. Furthermore, for any CO_2/H_2 feed ratio, DME yield increases with pressure and decreases with temperature, as expected [112].

Moreover, kinetic studies by Aguayo et al. [113] on one-step DME production using the hybrid catalyst CZA//γ-Al_2O_3 (where "//" denotes the combination of MeOH synthesis and dehydration functionalities) demonstrated that MeOH dehydration proceeds very rapidly, while the RWGS reaction remains at equilibrium. MeOH synthesis was identified as the rate-limiting step. Similar conclusions were drawn by Qin et al. [114], who employed a different hybrid catalyst, Cu–Fe_2O_3–ZrO_2//H-ZSM-5.

These findings highlight the multiple advantages of direct CO_2 hydrogenation to DME. However, achieving full selectivity toward DME appears challenging, if not impossible. As a result, despite the clear benefits of the one-step process, separation and recycle stages remain necessary to recover unconverted reactants and by-products.

The potential to enhance process performance through the *in situ* removal of H_2O from the reaction environment is particularly attractive, as in other hydrogenation processes where H_2O is a by-product. However, while the available scientific literature on SEMeOHS is already limited compared to its counterpart for methane production, the body of research focused on DME production is even scarcer (Table 2). Nevertheless, the few existing studies on this topic provide valuable insights and report promising results.

A first approach to this technology was presented in the simulation study by Iliuta et al. [98], in which a detailed model of a fixed bed reactor was developed, assuming the use of 4A zeolite for *in situ* water removal. The study focused on evaluating the influence of CO_2 content in the feed syngas on the performance of the SEDMES process. As expected, the results confirmed that water removal positively affects MeOH and DME yields, as well as DME selectivity. Notably, this enhancement becomes more significant as the CO_2 concentration in the feed increases—or conversely, as the CO concentration decreases. This behavior can be explained by considering the equilibrium of the main reactions involved in the process (i.e., Eqs. (3), (4), and (6)). A high CO_2 content leads to greater MeOH and, consequently, water production—especially due to the contribution of the RWGS reaction. Under non-sorption-enhanced conditions, this elevated water content limits MeOH dehydration. In contrast, a higher CO concentration in the feed reduces water formation via RWGS. Therefore, the benefits of water removal under sorption-enhanced conditions are more pronounced when the feed gas is richer in CO_2 (Fig. 22 [98]).

Van Kampen et al. [99] also developed a detailed process model, specifically investigating the impact of adsorption–regeneration cycle conditions on the performance of the SEDMES, assuming the use of 3A zeolite as the water sorbent. The simulation results demonstrated that, under sorption-enhanced conditions, a CO_2 conversion of 80% and a DME yield of 70% are achievable in a single-pass process. These findings underscore the significant potential of the one-pass configuration to reduce the need for downstream separation units and reactant recycling. A key parameter identified for process optimization was the effective management of the system's adsorption capacity, which depends heavily on the proper design of both adsorption and regeneration steps. Optimal adsorption was achieved at temperatures between 250 and 275 °C and pressures above 20 bar, with the reactor operating under near-isothermal conditions. For the regeneration phase, the best performance was obtained by combining temperature and pressure swing techniques.

The same research group also conducted an experimental campaign using a lab-scale high-pressure reactor, employing CZA for MeOH synthesis, γ-Al_2O_3 for MeOH dehydration, and 3A zeolite as a water sorbent. The experiments were performed at 25 bar and within a temperature range of 250–300 °C [101]. Interestingly, from a thermodynamic standpoint, carbon selectivity toward DME is not favorable under traditional conditions, with CO_2 being the predominant product. However, the introduction of a water sorbent significantly alters this behavior, as confirmed by both experimental results and process simulations (Fig. 23 [101]).

Furthermore, experimental results confirmed that careful management of the adsorption/regeneration cycles is a critical factor significantly impacting the overall process performance (Fig. 24 [102]). The findings showed that short cycles—with longer adsorption stages than regeneration stages—maximize DME productivity, though at the expense of DME selectivity. Conversely, higher selectivity can be achieved with longer overall cycles, particularly when the regeneration time exceeds that of adsorption.

It is important to note that the experimental and modeling studies on sorption-enhanced DME production discussed thus far have primarily focused on identifying and optimizing operating conditions. In contrast, the chemical investigation of catalysts and/or sorbents—such as material design, interaction mechanisms, or stability—has received little to no attention in this context.

3.3. Sorption-enhanced RWGS

For both MeOH and DME production, the RWGS reaction plays a significant role, acting as a critical factor influencing overall process performance. RWGS competes directly with MeOH synthesis, thereby reducing the selectivity toward the desired product—a phenomenon that becomes more pronounced under sorption-enhanced conditions. Similar considerations apply to DME production. More broadly, RWGS is relevant across all CO_2 hydrogenation processes within the context of energy transition. Its strategic importance also lies in its ability to generate CO, which serves as a versatile building block in the chemical industry for the synthesis of various organic and inorganic compounds, including as a precursor in plastics production.

From a thermodynamic standpoint, the RWGS reaction is endothermic (Eq. (3)) and it is unaffected by pressure variations (since it involves no net change in the number of gas-phase moles). The reaction is limited by the inherent chemical inertness of CO_2: At 600 °C, with a CO_2/H_2 feed ratio of 1, the equilibrium CO_2 conversion remains below 40%.

The removal of water from the reaction environment represents an attractive strategy for enhancing the performance of the

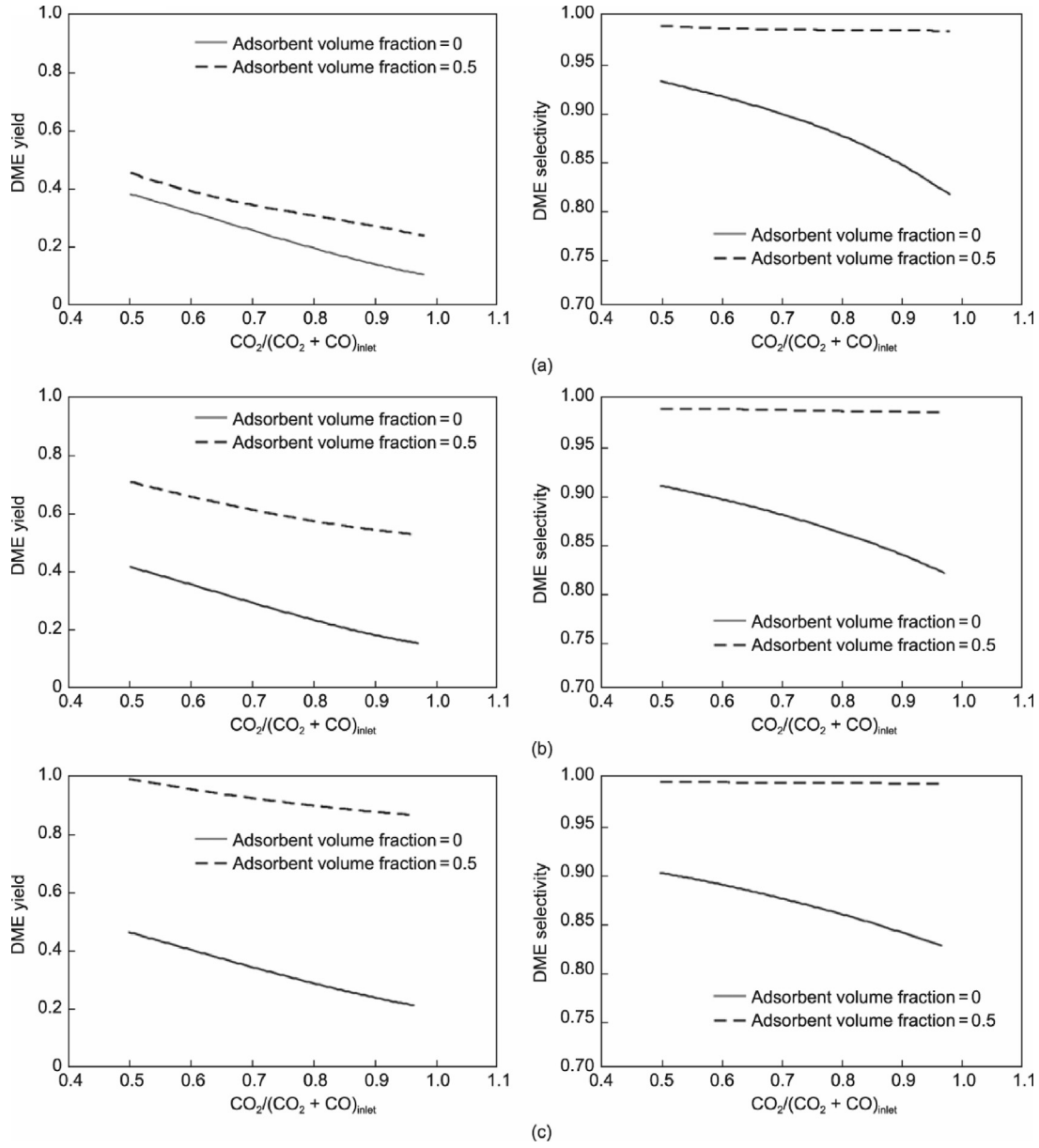

Fig. 22. Influence of feed CO_2 fraction on DME yield (on the left) and on DME selectivity (on the right) under H_2O removal conditions (at saturated H_2O adsorption capacity). Feed conditions: (a) H_2/CO_x = 1 (CO_2 + CO = 50%, H_2 = 50%); (b) H_2/CO_x = 1.5 (CO_2 + CO = 40%, H_2 = 60%); and (c) H_2/CO_x = 2 (CO_2 + CO = 33.3%, H_2 = 66.6%). Reproduced from Ref. [98] with permission.

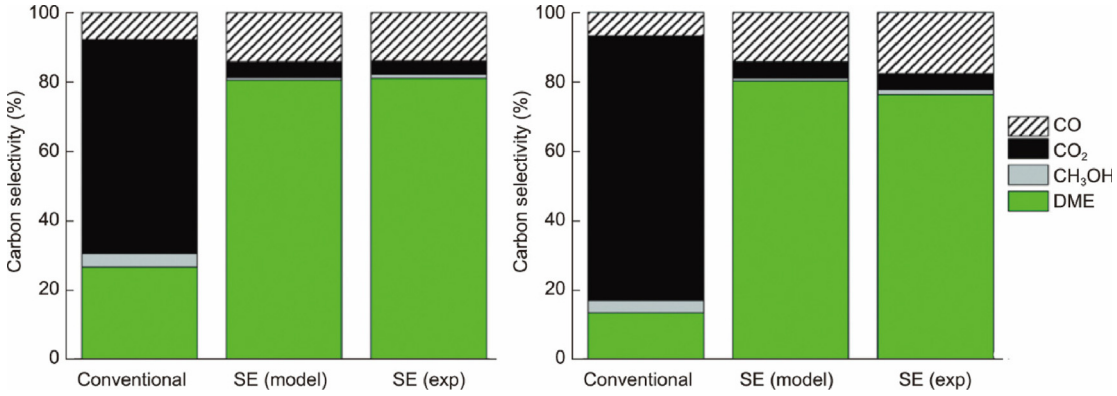

Fig. 23. Carbon selectivity for traditional direct synthesis of DME (thermodynamic equilibrium), for SEDMES model predictions, and SEDMES experimental results at 25 bar and 250 °C, with stoichiometric hydrogen, for: (left) CO_2:CO = 2:1 and (right): CO_2. Reproduced from Ref. [101] with permission.

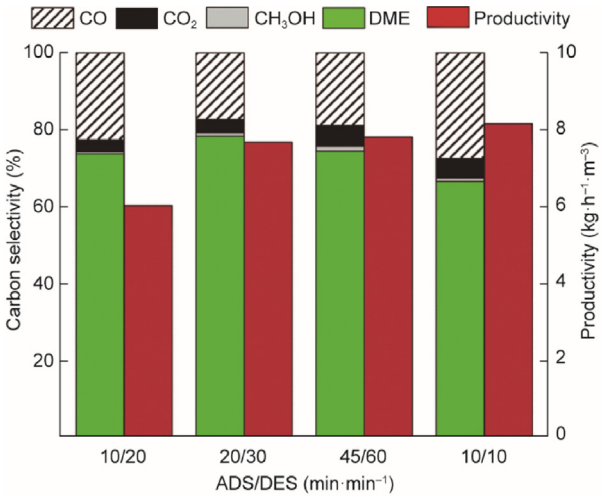

Fig. 24. Carbon selectivity and productivity vs ADS/DES time ratio (integration until 5% CO_2 breakthrough). Conditions: 250 °C, 25 bar, CO_2:CO = 2:1, stoichiometric hydrogen. Reproduced from Ref. [102] with permission.

process. One of the first studies on the implementation of SERWGS was conducted by Pieterse et al. [103], who performed an experimental investigation using a multi-column apparatus to test functional materials. The catalytic phase consisted of either Pt or Cu supported on two types of zeolites: 4A and 13X. The results demonstrated that all the bi-functional materials exhibited complete selectivity toward CO across a range of pressures (1–29 bar). Nevertheless, notable differences were observed among the materials. Regarding the catalytic phase, Pt showed higher activity than Cu, allowing for lower metal loading without compromising performance—thereby minimizing the risk of altering the zeolite structure. In contrast, the Cu/4A material exhibited very low reactivity, likely due to pore plugging, a problem not encountered with the Pt-based catalysts. As for the zeolite supports, 13X showed inferior performance compared to 4A, likely due to competitive adsorption between water and CO_2.

Similar results were reported by Desgagnés et al. [104,105], who investigated SERWGS using a 13X zeolite as the water sorbent, while a Cu-based upgraded slag oxides (UGSO) waste material served as the catalyst. The experimental campaign focused on evaluating the performance of bi-functional materials prepared through different methods: solid-state impregnation, wet impregnation, and deposition-precipitation. Additionally, the bi-functional materials' performance was compared to that of physical mixtures obtained by mechanical mixing (solid-state mixing and wet mixing) of the two active phases. Water adsorption capacity tests revealed that bi-functional materials suffer from pore plugging caused by catalyst deposition on the zeolite (Fig. 25 [104]).

To better understand the effect of catalyst addition on the zeolite, the authors also prepared bi-functional materials by depositing Cu—without UGSO—onto the 13X zeolite at different Cu loadings: 5, 7.5, 10, and 15 wt%. Fig. 26 [104] shows the adsorption capacity of these bi-functional materials, supported by porosimetric analysis data. The observed loss in water adsorption capacity was attributed not only to pore plugging but also to the weakening of acid sites caused by Cu deposition, which are primarily responsible for water adsorption. These findings suggest that using bi-functional materials with Cu as the catalyst phase may not be the optimal approach for implementing SERWGS.

Conversely, mechanically mixing the two active phases appeared to be a more effective strategy for the sorption-enhanced process. Experimental results from fixed bed reactor tests demonstrated that mechanical mixing via wet mixing led to a significant improvement, achieving an increase in CO production of about 50% at 250 °C with a catalyst-to-sorbent ratio of 20:80, compared to conditions without water removal (Fig. 27 [104]).

4. Conclusions and perspectives

This review showed that sorption-enhanced processes involving water vapor capture hold significant potential to improve catalytic hydrogenation reactions. Beyond increasing reactant conversion—and in some cases enhancing selectivity toward the desired product—these processes enable better control of reaction temperature and pressure conditions, offering substantial opportunities for energy efficiency improvements.

The literature overview covered SEM, SERWGS, SEDMES, and SEMeOHS, highlighting notable differences in their stages of technological development. For SEM and SERWGS research is most focused on the development of materials ensuring better performance and on new reactor concepts, while for SEDMES and SEMeOHS the focus is mostly on process optimization and scaling-up. Despite such differences, several common critical

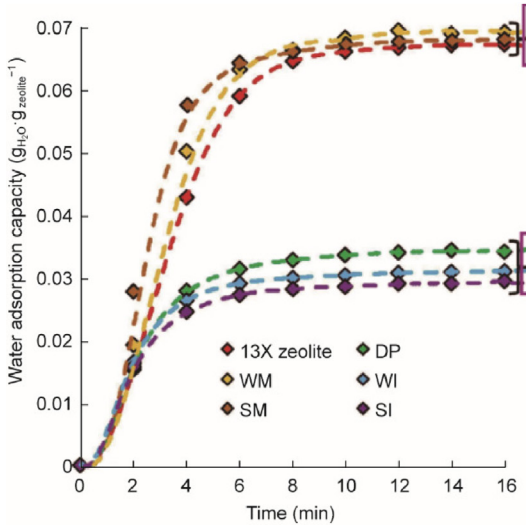

Material	BET surface area ($m^2 \cdot g^{-1}$)
13X zeolite	600
Solid state mixing (SM)	296
Wet mixing (WM)	310
Solid state impregnation (SI)	155
Wet impregnation (WI)	176
Deposition-precipitation (DP)	270
Cu-UGSO	47

Fig. 25. Effect of material preparation method on water adsorption capacity (with BET surface area). Experimental conditions: C/A ratio = 50/50, temperature = 250 °C, water partial pressure = 9.16 kPa. Reproduced from Ref. [104] with permission.

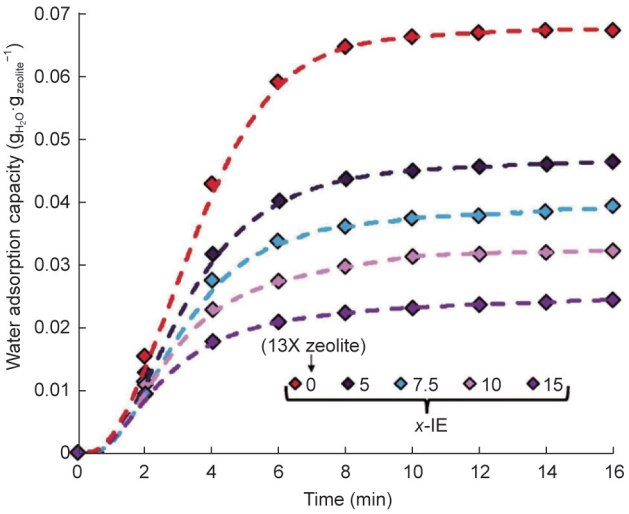

Material	BET surface area ($m^2 \cdot g^{-1}$)
13X zeolite	600
5-IE	526
7.5-IE	443
10-IE	340
15-IE	98

Fig. 26. Effect of the copper mass loading (*x*%) in the *x*-IE materials (Cu-doped 13X zeolites, prepared by ion exchange) on the water adsorption capacity (with BET surface area). The 0-IE sample refers to Cu-free 13X zeolite. Experimental conditions: temperature = 250 °C, water partial pressure = 9.16 kPa. Reproduced from Ref. [104] with permission.

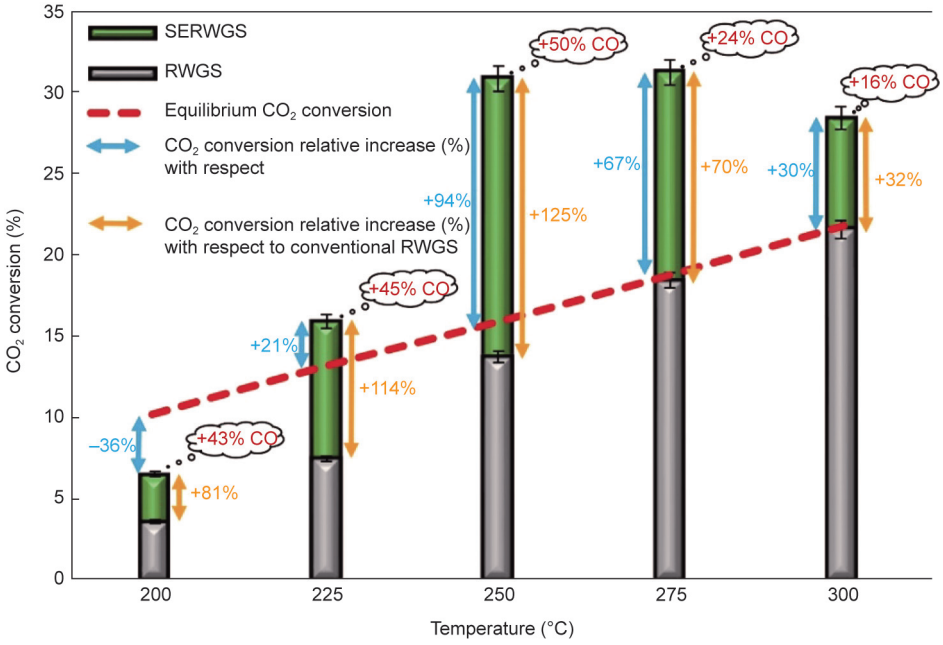

Fig. 27. Effect of temperature on the maximum CO_2 conversion in the SERWGS experiments, compared to equilibrium and conventional RWGS conversion. The numbers in the clouds refer to the additional relative amounts of CO produced in the SERWGS process compared to the RWGS process after 2 h on stream. Experimental conditions: hybrid material = WM, C/A ratio = 20/80, H_2/CO_2 feed ratio = 3, space velocity = 4800 $mL \cdot (g_{cat} \cdot h)^{-1}$, time on stream (TOS) = 2 h. Reproduced from Ref. [104] with permission.

challenges can be identified as key factors limiting the scale-up of these technologies to higher TRLs, as shown in Fig. 28.

One of the most challenging issues is the identification of suitable sorbent materials for H_2O capture. Such materials must effectively adsorb water at temperatures above 200 °C and exhibit high selectivity for H_2O, particularly in the presence of competing species such as CO_2 or the desired reaction product (methane, MeOH, DME, or CO). Additionally, they need to maintain stability over thousands of capture/regeneration cycles and be cost-effective for potential industrial applications. Furthermore, the sorbent should allow catalytic phases to be deposited within its pores without significantly compromising its water adsorption capacity, enabling the creation of efficient bi-functional catalysts. Currently, only zeolites partially meet these criteria, with temperature tolerance being the most critical limitation. Therefore, there is significant room for research focused on discovering new high-performance water sorbents or on improving the properties of existing ones.

Reactor configuration for sorption-enhanced processes is significantly more complex than for traditional catalytic hydrogenation reactions due to the need for periodic sorbent regeneration after saturation with water. Fixed bed reactors provide a compact and straightforward design. However, their operation is inherently discontinuous, requiring cyclic switching of gas flows and additional purge phases. Managing multiple transient reactors complicates operation and control, especially considering the highly exothermic nature of these reactions, which makes temperature control challenging in fixed beds. Alternatively, chemical looping

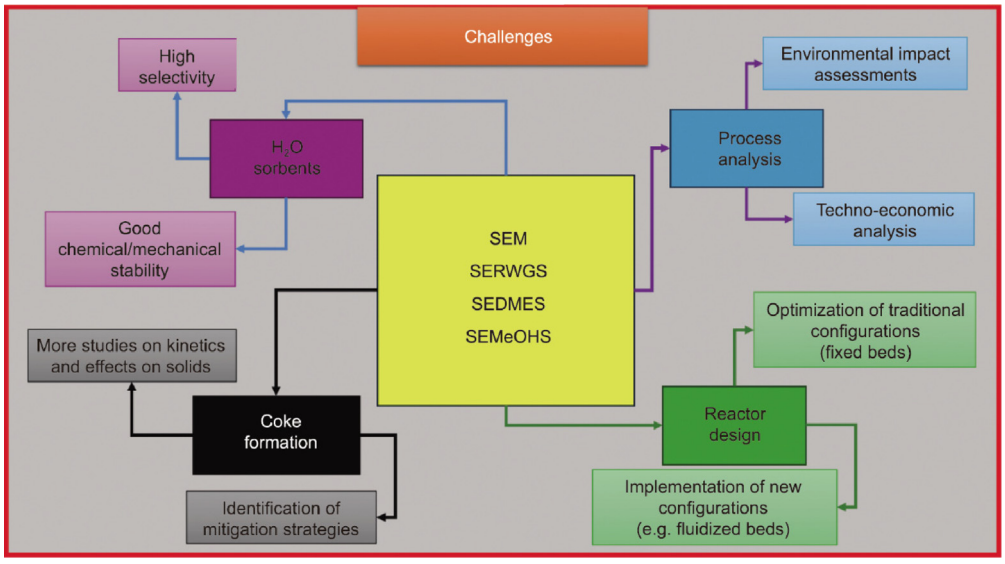

Fig. 28. Critical challenges limiting the scale-up of sorption-enhanced catalytic hydrogenation processes to industrial scale.

configurations based on interconnected fluidized bed reactors offer the potential for steady-state operation, continuous sorbent transfer and regeneration, and improved heat management. Nonetheless, research on applying fluidized bed systems to sorption-enhanced processes is scarce, and challenges related to solid circulation between reactors and the mechanical stability of sorbent/catalyst materials remain to be addressed. Therefore, substantial research efforts are needed to explore and develop these promising reactor configurations.

The risk of coke formation and deposition within the pores of sorbent and catalyst materials—and the resulting deactivation—appears to be elevated under sorption-enhanced conditions, as suggested primarily by thermodynamic analyses. However, experimental investigations into this critical issue remain limited. Future research should prioritize understanding and mitigating coke formation, as it directly impacts long-term catalyst and sorbent performance. Controlling the amount of water captured by the sorbent could play a key role in minimizing coke buildup, but currently, there is limited knowledge on the actual kinetics of coke formation across varying operating conditions, as well as on the long-term performance of the materials with this respect. Clarifying these issues is essential to inform sorbent and process design.

Finally, there is a notable lack of system integration, techno-economic and environmental impact assessments—such as LCA—focused on sorption-enhanced catalytic hydrogenation processes. Conducting such studies is crucial to comprehensively evaluate and compare the real benefits and potential trade-offs of sorption-enhanced technologies against conventional processes from economic, environmental, and sustainability perspectives. Such insights would guide informed decisions for scale-up and industrial implementation.

CRediT authorship contribution statement

Fiorella Massa: Writing – original draft, Methodology, Conceptualization. **Antonio Coppola:** Writing – original draft, Supervision, Methodology, Conceptualization. **Fabrizio Scala:** Writing – review & editing, Supervision, Project administration, Methodology, Funding acquisition, Conceptualization.

Declaration of competing interest

The authors declare that they have no known competing financial interests or personal relationships that could have appeared to influence the work reported in this paper.

Acknowledgments

Project funded under the National Recovery and Resilience Plan, Mission 4 Component 2 Investment 1.3, Concession Decree (1561 of 11.10.2022) of Ministero dell'Università e della Ricerca (MUR); funded by the European Union—NextGenerationEU (PE0000021), CUP: B53C22004060006, CUP: E63C22002160007. Fiorella Massa acknowledges funding from the European Union—NextGenerationEU under the National Recovery and Resilience Plan, Mission 04 Component 2 Investment 3.1 (IR0000027-CUP: B33C22000710006-iENTRANCE@ENL). Fabrizio Scala acknowledges funding from REFRESH, CZ.10.03.01/00/22_003/0000048 via the Operational Programme Just Transition, and from Ministero dell'Ambiente e della Sicurezza Energetica (MASE), project e-KEROMETH, n. RSH2A_000032, PNRR—Mission 2.

References

[1] Climate change. Washington, DC: National Aeronautics and Space Administration; 2025 Sep 16 [cited 2025 May 8]. Available from: https://science.nasa.gov/climate-change/.
[2] Emissions gap report 2024. Report. Nairobi: United Nations Environment Programme; 2024.
[3] World energy outlook. Report. Paris: International Energy Agency; 2024.
[4] Trends in CO_2, CH_4, N_2O, SF_6. Report. Boulder: National Oceanic & Atmospheric Administration Global Monitoring Laboratory; 2024.
[5] The Paris Agreement. Report. Bonn: United Nations Framework Convention on Climate Change; 2015.
[6] Synthesis report. Report. Geneva: Intergovernmental Panel on Climate Change; 2024.
[7] Conference of the Parties (COP). Report. Bonn: United Nations Framework Convention on Climate Change.
[8] Podder J, Patra BR, Pattnaik F, Nanda S, Dalai AK. A review of carbon capture and valorization technologies. Energies 2023;16(6):2589.
[9] Zhu Q. Developments on CO_2-utilization technologies. Clean Energy 2019;3(2):85–100.
[10] Turgut MG. Carbon dioxide emissions, capture, storage and utilization: review of materials, processes and technologies. Prog Energy Combust Sci 2022;89:100965.
[11] CCUS in clean energy transitions. Report. Paris: International Energy Agency; 2020.

[12] Valluri S, Claremboux V, Kawatra S. Opportunities and challenges in CO_2 utilization. J Environ Sci 2022;113:322–44.
[13] Gowd SC, Ganeshan P, Vigneswaran VS, Hossain M, Kumar D, Rajendran K, et al. Economic perspectives and policy insights on carbon capture, storage, and utilization for sustainable development. Sci Total Environ 2023;883:163656.
[14] Putting CO_2 to use. Report. Paris: International Energy Agency; 2019.
[15] Hoang AT, Sirohi R, Pandey A, Nižetić S, Lam SS, Chen WH, et al. Biofuel production from microalgae: challenges and chances. Phytochem Rev 2023;22(4):1089–126.
[16] Woodall CM, McQueen N, Pilorgé H, Wilcox J. Utilization of mineral carbonation products: current state and potential. Greenh Gases Sci Technol 2019;9(6):1096–113.
[17] Divya B, Panchamoorthy S, Nagarajan L, Hun-Soo B. An overview of technologies for capturing, storing, and utilizing carbon dioxide: technology readiness, large-scale demonstration, and cost. Chem Eng J 2024;491:151998.
[18] Chauvy R, Meunier N, Thomas D, De Weireld G. Selecting emerging CO_2 utilization products for short- to mid-term deployment. Appl Energy 2019;236:662–80.
[19] Soltani SM, Lahiri A, Bahzadb H, Cloughd P, Gorbounova M, Yan Y. Sorption-enhanced steam methane reforming for combined CO_2 capture and hydrogen production: a state-of-the-art review. Carbon Capture Sci Technol 2021;1:100003.
[20] Abdin Z, Zafaranloo A, Rafiee A, Mérida W, Lipiński W, Khalilpour KR. Hydrogen as an energy vector. Renew Sustain Energy Rev 2020;120:109620.
[21] Global hydrogen review. Report. Paris: International Energy Agency; 2024.
[22] Patel GH, Havukainen J, Horttanainen M, Soukka R, Tuomaala M. Climate change performance of hydrogen production based on life cycle assessment. Green Chem 2024;26(2):992–1006.
[23] Alasali F, Abuashour MI, Hammad W, Almomani D, Obeidat AM, Holderbaum W. A review of hydrogen production and storage materials for efficient integrated hydrogen energy systems. Energy Sci Eng 2024;12(5):1934–68.
[24] Kumar SS, Himabindu V. Hydrogen production by PEM water electrolysis—a review. Mater Sci Energy Technol 2019;2(3):442–54.
[25] Agyekum EB, Nutakor C, Agwa AM, Kamel S. A critical review of renewable hydrogen production methods: factors affecting their scale-up and its role in future energy generation. Membranes 2022;12(2):173.
[26] Tawalbeh M, Javed RMN, Al-Othman A, Almomani F. The novel contribution of non-noble metal catalysts for intensified carbon dioxide hydrogenation: recent challenges and opportunities. Energy Convers Manage 2023;279:116755.
[27] Vieira LH, Rasteiro LF, Santana CS, Catuzo GL, da Silva AHM, Assaf JM, et al. Noble metals in recent developments of heterogeneous catalysts for CO_2 conversion processes. ChemCatChem 2023;15(14):e202300493.
[28] Gao D, Li W, Wang H, Wang G, Cai R. Heterogeneous catalysis for CO_2 conversion into chemicals and fuels. Trans Tianjin Univ 2022;28:245–64.
[29] Vu TTN, Desgagnés A, Iliuta MC. Efficient approaches to overcome challenges in material development for conventional and intensified CO_2 catalytic hydrogenation to CO_2 methanol, and DME. Appl Catal A Gen 2021;617:118119.
[30] Álvarez A, Bansode A, Urakawa A, Bavykina AV, Wezendonk TA, Makkee M, et al. Challenges in the greener production of formates/formic acid, methanol, and DME by heterogeneously catalyzed CO_2 hydrogenation processes. Chem Rev 2017;117(14):9804–38.
[31] Iliuta MC. Intensified processes for CO_2 capture and valorization by catalytic conversion. Chem Eng Process 2024;205:109995.
[32] Boon J. Sorption-enhanced reactions as enablers for CO_2 capture and utilization. Curr Opin Chem Eng 2023;40:100919.
[33] Faria C, Rocha C, Miguel C, Rodrigues A, Madeira LM. Process intensification concepts for CO_2 methanation—a review. Fuel 2025;386:134269.
[34] van Kampen J, Boon J, van Berkel F, Vente J, van Sint AM. Steam separation enhanced reactions: review and outlook. Chem Eng J 2019;374:1286–303.
[35] Carvill BT, Hufton JR, Anand M, Sircar S. Sorption-enhanced reaction process. AIChE J 1996;42(10):2765–72.
[36] Ghodhbene M, Bougie F, Fongarland P, Iliuta MC. Hydrophilic zeolite sorbents for In-situ water removal in high temperature processes. Can J Chem Eng 2017;95(10):1842–9.
[37] Wei L, Haije W, Grénman H, de Jong W. Sorption enhanced catalysis for CO_2 hydrogenation towards fuels and chemicals with focus on methanation. In: Cesario MR, De Macedo DA, editors. Heterogeneous catalysis. Amsterdam: Elsevier; 2022. p. 95–119.
[38] Rönsch S, Schneider J, Matthischke S, Schlüter M, Götz M, Lefebvre J, et al. Review on methanation—from fundamentals to current projects. Fuel 2016;166:276–96.
[39] Biswas S, Kulkarni AP, Giddey S, Bhattacharya S. A review on synthesis of methane as a pathway for renewable energy storage with a focus on solid oxide electrolytic cell-based processes. Front Energy Res 2020;8:570112.
[40] Sabatier P, Senderens JB. New methane synthesis. J Chem Soc 1902;82:333–7.
[41] Mills GA, Steffgen FW. Catalytic methanation. Catal Rev Sci Eng 1974;8 (1):159–210.
[42] Bartholomew CH. Mechanisms of catalyst deactivation. Appl Catal A Gen 2001;212(1–2):17–60.
[43] Xu J, Froment GF. Methane steam reforming, methanation and water–gas shift: intrinsic kinetics. AIChE J 1989;35(1):88–96.
[44] Gao J, Liu Q, Gu F, Liu B, Zhong Z, Su F. Recent advances in methanation catalysts for the production of synthetic natural gas. RSC Adv 2015;5 (29):22759–76.
[45] Frontera P, Macario A, Ferraro M, Antonucci P. Supported catalysts for CO_2 methanation: a review. Catalysts 2017;7(2):59.
[46] Hubble RA, Lim JY, Dennis JS. Kinetic studies of CO_2 methanation over a Ni/g-Al_2O_3 catalyst. Faraday Discuss 2016;192:529–44.
[47] Kopyscinski J, Schildhauer TJ, Biollaz SMA. Production of synthetic natural gas (SNG) from coal and dry biomass—a technology review from 1950 to 2009. Fuel 2010;89(8):1763–83.
[48] Hervy M, Maistrello J, Brito L, Rizand M, Basset E, Kara Y, et al. Power-to-gas: CO_2 methanation in a catalytic fluidized bed reactor at demonstration scale, experimental results and simulation. J CO_2 Util 2021;50:101610.
[49] Koytsoumpa EI, Karellas S. Equilibrium and kinetic aspects for catalytic methanation focusing on CO_2 derived substitute natural gas (SNG). Renew Sustain Energy Rev 2018;94:536–50.
[50] Gao J, Wan Y, Ping Y, Hu D, Xu G, Gu F, et al. A thermodynamic analysis of methanation reactions of carbon oxides for the production of synthetic natural gas. RSC Adv 2012;2(6):2358–68.
[51] Frick V, Brellochs J, Specht M. Application of ternary diagrams in the design of methanation systems. Fuel Process Technol 2014;118:156–60.
[52] Swapnesh A, Srivastava VC, Mall ID. Comparative study on thermodynamic analysis of CO_2 utilization reactions. Chem Eng Technol 2014;37 (10):1765–77.
[53] Faria AC, Miguel CV, Madeira LM. Thermodynamic analysis of the CO_2 methanation reaction with *in situ* water removal for biogas upgrading. J CO_2 Util 2018;26:271–80.
[54] Massa F, Coppola A, Scala F. A thermodynamic study of sorption-enhanced CO_2 methanation at low pressure. J CO_2 Util 2020;35:176–84.
[55] Hashemi SE, Lien KM, Hillestad M, Schnell SK, Austbø B. Thermodynamic insight in design of methanation reactor with water removal considering nexus between CO_2 conversion and irreversibilities. Energies 2021;14 (23):7861.
[56] Borgschulte A, Gallandat N, Probst B, Suter R, Callini E, Ferri D, et al. Sorption enhanced CO_2 methanation. Phys Chem Chem Phys 2013;15 (24):9620–5.
[57] Borgschulte A, Callini E, Stadie N, Arroyo Y, Rossell MD, Erni R, et al. Manipulating the reaction path of the CO_2 hydrogenation reaction in molecular sieves. Catal Sci Technol 2015;5(9):4613–21.
[58] Borgschulte A, Delmelle R, Duarte RB, Heel A, Boillat P, Lehmann E. Water distribution in a sorption enhanced methanation reactor by time resolved neutron imaging. Phys Chem Chem Phys 2016;18(26):17217–23.
[59] Walspurger S, Elzinga GD, Dijkstra JW, Saric M, Haije WG. Sorption enhanced methanation for substitute natural gas production: experimental results and thermodynamic considerations. Chem Eng J 2014;242:379–86.
[60] Delmelle R, Duarte RB, Franken T, Burnat D, Holzer L, Borgschulte A, et al. Development of improved nickel catalysts for sorption enhanced CO_2 methanation. Int J Hydrogen Energy 2016;41(44):20185–91.
[61] Delmelle R, Terreni J, Remhof A, Heel A, Proost J, Borgschulte A. Evolution of water diffusion in a sorption-enhanced methanation catalyst. Catalysts 2018;8(9):341.
[62] Agirre I, Acha E, Cambra JF, Barrio VL. Water sorption enhanced CO_2 methanation process: optimization of reaction conditions and study of various sorbents. Chem Eng Sci 2021;237:116546.
[63] Wei L, Azad H, Haije W, Grenman H, de Jong W. Pure methane from CO_2 hydrogenation using a sorption enhanced process with catalyst/zeolite bifunctional materials. Appl Catal B 2021;297:120399.
[64] Coppola A, Massa F, Salatino P, Scala F. Fluidized bed CaO hydration–dehydration cycles for application to sorption-enhanced methanation. Combust Sci Technol 2019;191(9):1724–33.
[65] Coppola A, Massa F, Salatino P, Scala F. Evaluation of two sorbents for the sorption-enhanced methanation in a dual fluidized bed system. Biomass Convers Biorefin 2021;11(1):111–9.
[66] García YC, Martínez I, Grasa G. Determination of the hydration and carbonation kinetics of CaO for low-temperature applications. Chem Eng Sci 2024;295:120146.
[67] Gómez L, Martínez I, Navarro MV, García T, Murillo R. Sorption-enhanced CO and CO_2 methanation (SEM) for the production of high purity methane. Chem Eng J 2022;440:135842.
[68] Gómez L, Martínez I, Navarro MV, Murillo R. Selection and optimisation of a zeolite/catalyst mixture for sorption-enhanced CO_2 methanation (SEM) process. J CO_2 Util 2023;77:102611.
[69] Gómez L, Nguyen-Quang M, Azzolina-Jury F, Martínez I, Murillo R. *In-situ* FTIR analysis on conventional and sorption-enhanced methanation (SEM) processes over Ni, Rh, and Ru-based catalyst systems. Appl Catal A Gen 2024;678:119733.
[70] Gómez L, Martínez I, Grasa G, Murillo R. Experimental demonstration of a sorption-enhanced methanation (SEM) cyclic process on a lab-scale TRL-3 fixed bed reactor. Chem Eng J 2024;491:151744.
[71] Gómez L, Martínez I, Grasa G, Murillo R. Different feed mixtures for the sorption-enhanced methanation (SEM) process on a lab-scale TRL-3 fixed-bed reactor. Energy Fuels 2024;38(18):17834–46.
[72] Mercader VD, Durán P, Aragüés-Aldea P, Francés E, Herguido J, Peña JA. Biogas upgrading by intensified methanation (SESaR): reaction plus water adsorption—desorption cycles with Ni-Fe/Al_2O_3 catalyst and LTA 5A zeolite. Catal Today 2024;433:114667.

[73] Kiefer F, Nikolic M, Borgschulte A, Eggenschwile PD. Sorption-enhanced methane synthesis in fixed-bed reactors. Chem Eng J 2022;449:137872.
[74] Barbaresi A, Morini M, Gambarotta A, Kiefer F, Eggenschwiler PD. Modeling sorption-enhanced methane synthesis for system control and operation. Renew Energy 2024;232:121020.
[75] Cañada-Barcala A, Larriba M, Águeda Maté VI, Delgado Dobladez JA. CO_2 methanation enhanced with a cyclic SERP process using a commercial Ni-based catalyst mixed with 3A zeolite as adsorbent. Chem Eng J 2023;461:141897.
[76] Cañada-Barcala A, Larriba M, Águeda Maté VI, Delgado Dobladez JA. Synthetic natural gas production through biogas methanation using a sorption-enhanced reaction process. Separ Purif Tech 2024;331:125714.
[77] Coppola A, Massa F, Scala F. Simulation of a sorption-enhanced methanation process with CaO in a dual interconnected fluidized bed system. Fuel 2023;339:127374.
[78] Massa F, Scala F, Coppola A. Simulation of biogas upgrading by sorption-enhanced methanation with CaO in a dual interconnected fluidized bed system. Processes 2023;11(11):3218.
[79] Bareschino P, Piso G, Pepe F, Tregambi C, Mancusi E. Numerical modelling of a sorption-enhanced methanation system. Chem Eng Sci 2023;277:118876.
[80] Mancusi E, Piso G, Shah HH, Pepe F, Tregambi C, Bareschino P. Modelling of a continuous sorption-enhanced methanation process in an adiabatic packed-bed reactor system. Chem Eng Sci 2025;301:120800.
[81] Chirone R, Paulillo A, Coppola A, Scala F. Carbon capture and utilization via calcium looping, sorption enhanced methanation and green hydrogen: a techno-economic analysis and life cycle assessment study. Fuel 2022;328:125255.
[82] Sheldon D. Methanol production—a technical history. Johns Matthey Technol Rev 2017;61(3):172–82.
[83] Olah GA, Prakash GKS, Goeppert A. Anthropogenic chemical carbon cycle for a sustainable future. J Am Chem Soc 2011;133(33):12881–98.
[84] Olah GA. Beyond oil and gas: the methanol economy. Angew Chem Int Ed 2005;44(18):2636–9.
[85] Olah GA, Goeppert A, Prakash GKS. Chemical recycling of carbon dioxide to methanol and dimethyl ether: from greenhouse gas to renewable, environmentally carbon neutral fuels and synthetic hydrocarbons. J Org Chem 2009;74(2):487–98.
[86] Ganesh I. Conversion of carbon dioxide into methanol—a potential liquid fuel: fundamental challenges and opportunities (a review). Renew Sustain Energy Rev 2014;31:221–57.
[87] Zachopoulos A, Heracleous E. Overcoming the equilibrium barriers of CO_2 hydrogenation to methanol via water sorption: a thermodynamic analysis. J CO_2 Util 2017;21:360–7.
[88] Maksimov P, Laari A, Ruuskanen V, Koiranen T, Ahola J. Methanol synthesis through sorption enhanced carbon dioxide hydrogenation. Chem Eng J 2021;418:129290.
[89] Pascual-Muñoz G, Calero-Berrocal R, Larriba M, Ismael Águeda V, Antonio DJ. Experimental PSA reactor for methanol-enhanced production VIA CO_2 hydrogenation. Separ Purif Tech 2024;351:128030.
[90] Heracleous E, Koidi V, Lappas AA. Experimental investigation of sorption-enhanced CO_2 hydrogenation to methanol. ACS Sustain Chem Eng 2023;11(26):9684–95.
[91] Pascual-Muñoz G, Cañada-Barcala A, Alberola R, Álvarez-Torrellas S, Larriba M, Águeda VI, et al. Improvement of methanol production from carbon dioxide and hydrogen by a sorption enhanced reaction process. Chem Eng Trans 2021;86:1081–6.
[92] Heracleous E, Koidi V, Lappas AA. Effect of zeolite type in sorption-enhanced CO_2 hydrogenation to methanol. Chem Eng J 2024;502:157846.
[93] Terreni J, Trottmann M, Franken T, Heel A, Borgschulte A. Sorption-enhanced methanol synthesis. Energy Technol 2019;7(4):1–9.
[94] Pascual-Muñoz G, Calero-Berrocal R, Larriba M, Águeda VI, Delgado JA. Influence of sodium and potassium proportion on the adsorption of methanol and water on LTA zeolites at high temperature. Microporous Mesoporous Mater 2023;360:112669.
[95] Nikolic M, Daemen L, Ramirez-Cuesta AJ, Xicohtencatl RB, Cheng Y, Putnam ST, et al. Neutron insights into sorption enhanced methanol catalysis. Top Catal 2021;64(9–12):638–43.
[96] Nieminen H, Maksimov P, Laari A, Väisänen V, Vuokila A, Huuhtanen M, et al. Process modelling and feasibility study of sorption-enhanced methanol synthesis. Chem Eng Process 2022;179:109052.
[97] Maksimov P, Nieminen H, Laari A, Koiranen T. Sorption enhanced carbon dioxide hydrogenation to methanol: process design and optimization. Chem Eng Sci 2022;252:117498.
[98] Iliuta I, Iliuta MC, Larachi F. Sorption-enhanced dimethyl ether synthesis—multiscale reactor modeling. Chem Eng Sci 2011;66(10):2241–51.
[99] Van Kampen J, Boon J, Vente J, Van Sint Annaland M. Sorption enhanced dimethyl ether synthesis for high efficiency carbon conversion: modelling and cycle design. J CO_2 Util 2020;37:295–308.
[100] Altinsoy NS, Avci AK. Sorption enhanced DME synthesis by one-step CO_2 hydrogenation. Chem Eng Process 2024;203:109874.
[101] Van Kampen J, Boon J, Vente J, Van Sint AM. Sorption enhanced dimethyl ether synthesis under industrially relevant conditions: experimental validation of pressure swing regeneration. React Chem Eng 2021;6(2):244–57.
[102] Van Kampen J, Booneveld S, Boon J, Vente J, Van Sint AM. Experimental validation of pressure swing regeneration for faster cycling in sorption enhanced dimethyl ether synthesis. Chem Commun 2020;56(88):13540–2.
[103] Pieterse JAZ, Elzinga GD, Booneveld S, van Kampen J, Boon J. Reactive water sorbents for the sorption-enhanced reverse water–gas shift. Catal Lett 2022;152(2):460–6.
[104] Desgagnés A, Iliuta MC. Intensification of CO_2 hydrogenation by *in-situ* water removal using hybrid catalyst-adsorbent materials: effect of preparation method and operating conditions on the RWGS reaction as a case study. Chem Eng J 2023;454:140214.
[105] Desgagnés A, Iliuta I, Iliuta MC. Sorption-enhanced intensified CO_2 hydrogenation via reverse water–gas shift reaction: kinetics and modelling. Chem Eng J 2024;494:152052.
[106] Xu M, Lunsford JH, Goodman DW, Bhattacharyya A. Synthesis of dimethyl ether (DME) from methanol over solid-acid catalysts. Appl Catal A 1997;149(2):289–301.
[107] Stöcker M. Methanol-to-hydrocarbons: catalytic materials and their behavior. Microporous Mesoporous Mater 1999;29(1–2):3–48.
[108] Peinado C, Liuzzi D, Sluijter SN, Skorikova G, Boon J, Guffanti S, et al. Review and perspective: next generation DME synthesis technologies for the energy transition. Chem Eng J 2024;479:147494.
[109] Azizi Z, Rezaeimanesh M, Tohidian T, Rahimpour MR. Dimethyl ether: a review of technologies and production challenges. Chem Eng Proc 2014;82:150–72.
[110] Cai M, Palčić A, Subramanian V, Moldovan S, Ersen O, Valtchev V, et al. Direct dimethyl ether synthesis from syngas on copper-zeolite hybrid catalysts with a wide range of zeolite particle sizes. J Catal 2016;338:227–38.
[111] Bonura G, Cordaro M, Cannilla C, Mezzapica A, Spadaro L, Arena F, et al. Catalytic behaviour of a bifunctional system for the one step synthesis of DME by CO_2 hydrogenation. Catal Today 2014;228:51–7.
[112] Shen WJ, Jun KW, Choi HS, Lee KW. Thermodynamic investigation of methanol and dimethyl ether synthesis from CO_2 hydrogenation. Korean J Chem Eng 2000;17:210–6.
[113] Aguayo AT, Ereña J, Mier D, Arandes JM, Olazar M, Bilbao J. Kinetic modeling of dimethyl ether synthesis in a single step on a CuO–ZnO–Al_2O_3/γ-Al_2O_3 catalyst. Ind Eng Chem Res 2007;46(17):5522–30.
[114] Qin Z, Su T, Ji H, Jiang Y, Liu R, Chen J. Experimental and theoretical study of the intrinsic kinetics for dimethyl ether synthesis from CO2 over Cu–Fe–Zr/HZSM-5. AIChE J 2015;61(5):1613–27.